This is a peer-reviewed, accepted author manuscript of the following research chapter: Brown, C., McGlone, T., & Florence, A. (2017). Continuous crystallisation. In P. Kleinebudde, J. Khinast, & J. Rantanen (Eds.), *Continuous Manufacturing of Pharmaceuticals* (pp. 169-226). John Wiley & Sons Inc..

1 Continuous Crystallisation

Cameron Brown[a], Thomas McGlone[a] and Alastair Florence[a]

[a] Centre for Innovative Manufacturing in Continuous Manufacturing and Crystallisation (CMAC), University of Strathclyde, Technology Innovation Centre, 99 George Street, Glasgow, G1 1RD, U.K.

1.1 Introduction

Although crystallisation in pharmaceutical manufacturing is traditionally carried out as a batch operation, with the drive towards implementing continuous manufacturing of pharmaceuticals there is increased interest in developing and applying approaches for continuous crystallisation [1, 2]. Indeed, the potential to directly connect multiple process stages as part of an integrated end-to-end process chain including a continuous crystallisation step has been demonstrated for the manufacture of aliskiren hemifumarate tablets [3] and in a compact reconfigurable platform for a range of liquid dosage APIs [4]. Crystallisation is a key operation for the purification and isolation of active pharmaceutical ingredients (APIs) from solution mixtures to produce pure drug substance in a stable, solid form suitable for subsequent formulation and processing. Crystallisation is therefore a critical stage in controlling the physical properties of the solid material [5, 6]. For pharmaceuticals, achieving high levels of chemical purity of crystallised or precipitated particles is an essential requirement. However, a given API can also show a range of variability in crystalline form (polymorph, solvate, salt, co-crystal), crystal size, size distribution and shape that can have significant effects on processing performance and product stability [7]. Consequently, robust continuous crystallisation processes are required that can achieve the target particle attributes consistently and avoid uncontrolled variation in quality and performance. However, despite the widespread application of crystallisation in fine chemical and pharmaceutical production, it still remains relatively poorly understood. Hence the development of consistent and robust continuous crystallisation processes requires systematic and rigorous approaches to identify and control the complex physical transformations that take place within a multicomponent, multiphase process environment.

Pharmaceutical materials also frequently display other challenging physical properties that need to be managed during crystallisation. These include the tendency of low symmetry crystals to adopt extreme morphologies [8], the occurrence of attrition during processing [9] due to relatively fragile crystal mechanical properties [10] as well as a tendency for crystals to agglomerate [11, 12]. Specific process requirements are dictated by the particular physical properties of the system and an overall understanding of the interactions between material properties, process conditions and particle attributes is therefore necessary. In principle, this can be achieved by the implementation of Quality by Design (QbD) principles during process development to establish a rigorous understanding of the process and acceptable operating ranges to

achieve the required performance [13, 14]. Processes must also be designed to meet economic and sustainability requirements.

Continuous crystallisation technologies offer considerable flexibility over the control of crystallisation, allowing each stage of the process to be physically separated and controlled (Table 1.1). This separation of the key transformations along with a relative reduction in the volume of material to be controlled, allows for closer control over the conditions governing the individual transformations at each stage that dictate the final crystal size distribution and product quality. For example, primary nucleation processes typically require higher levels of supersaturation than crystal growth. Thus control can be achieved in multiple vessels for example with primary nucleation being driven in a stirred tank operating at high supersaturation, and subsequent vessels operating at lower supersaturations to achieve controlled growth rates and effective rejection of impurities [15]. Hence a variety of process configurations have been demonstrated on different platforms and systems.

Table 1.1. Key stages, aims and consideration for selection of conditions during continuous crystallisation

1) Mixing	2) Nucleation	3) Growth	4) Filter/wash/dry
Required to: • Produce consistent composition • Control crystallisation driving force • Influence flow rate, shear-kinetic effects • Consistent suspension of seed and product	**Controlled via:** • Supersaturation • High shear • External fields, e.g. ultrasound, non-photochemical laser induced nucleation • Seed. Seeds produced via dry milling, wet media milling, precipitation, recycle, dissolution, spray drying or secondary nucleation **Controlled to avoid:** • Fouling • Agglomeration • Dissolution • Crystalline form transformation(s)	**Controlled via:** • Supersaturation (typically low) via cooling, anti-solvent, evaporation • Effective heat/mass transfer **Ensures:** • Efficient desupersaturation **Controlled to avoid:** • Fouling • Agglomeration • Attrition (particle breakage) • Dissolution • Crystalline form transformation(s)	**Required to:** • Create filter cake • Remove mother liquor and impurities • Maintain particle attributes **Controlled to avoid:** • Agglomeration • Attrition (particle breakage)

Continuous crystallisation has been implemented for many decades in other manufacturing sectors, typically for large volume commodity chemicals, and offers a range of potential advantages [16, 17] including lower operating and capital costs, reduced down time and more efficient use of energy and materials. Cooling and anti-solvent crystallisation are commonly used in industrial applications and can be readily implemented in continuous. The aim is to follow a controlled trajectory through the solubility phase diagram (section 1.2).

Using seeding combined with PAT enables a direct supersaturation control approach that allows the system to optimize growth whilst avoiding uncontrolled primary nucleation and broadening of the particle size distribution (PSD) or the unexpected appearance of different crystalline forms. The uncontrolled generation of particles via secondary nucleation and attrition (particle breakage) can also impact on the PSD though may be minimised by maintaining control over supersaturation and controlling shear forces across the process stages. Approaches for dealing with fines that involve temperature cycling either in a recycle loop or spatially along the crystalliser may also be applied [15].

Continuous operation of crystallisation processes under a controlled state offers a number of potential advantages for the control of particle attributes:

- Accurate control of purity, yield, crystalline form (polymorph, salt, solvate, co-crystal), particle size distribution (PSD) and particle shape or morphology.
- Control of particle size yielding consistent slurry and powder properties improving filtration, drying and bulk flow/formulation properties
- Growth of targeted PSD enables opportunity to eliminate post-crystallisation milling
- Suitability for application of on-line sensors for real-time process monitoring and control
- Elimination of batch-to-batch variability
- Scalability of processes through extending operation times, equipment scale-up as well as scale-out/numbering up approaches
- Adaptability of technologies for multiple products including ability to reconfigure modular platforms to deal with different physical properties.

Given this range of capabilities to support advanced pharmaceutical manufacturing approaches, it is unsurprising that continuous crystallisation has been investigated in a range of platforms [18] including mixed suspension mixed product removal (MSMPR) [19-22] and plug flow reactors (PFRs) [23] including oscillatory flow reactors (OFR) [16, 24, 25] (Figure 1.1). A wide array of implementations and technologies have been successfully demonstrated including impinging jet mixers for reactive crystallisation or precipitation [26] often operated in conjunction with MSMPRs, static mixers for anti-solvent crystallisation [27] and segmented (slug) flow reactors [28]. The operation of continuous crystallisations in supersaturated environments for extended periods can also pose challenges including instabilities introduced by variations in services and fouling or encrustation that need to be managed. Fouling or encrustation of vessels, feed lines, or PAT probes under elevated supersaturation and/or solid loadings is a particular issue where extended operation of the process is required, and can lead to disruption of flow, degradation of heat transfer and blockage of reactor channels. Indeed, it can be expected to occur eventually even where crystallisers operated at low supersaturation and approaches to prevent or mitigate accumulation are essential. Localized heating, choice of materials of construction and coatings or the use of ultrasound may be of benefit

alongside periodic, scheduled, off-line solvent cleanout. Multi-vessel CSTR cascades can be operated with individual vessel cleanout during continuous operations. The use of ultrasound as an external field, for example, has been shown to be effective in reducing fouling during the continuous crystallisation of adipic acid [29]. For the most part, each of these types of crystalliser is capable of operating with or without seeding and in cooling, anti-solvent and reactive modes. Additional features such as ultrasound, static mixing or flow oscillations and agitated cell and tubular reactor configurations have also been applied to provide additional flexibility [16, 19, 23, 27, 30-32].

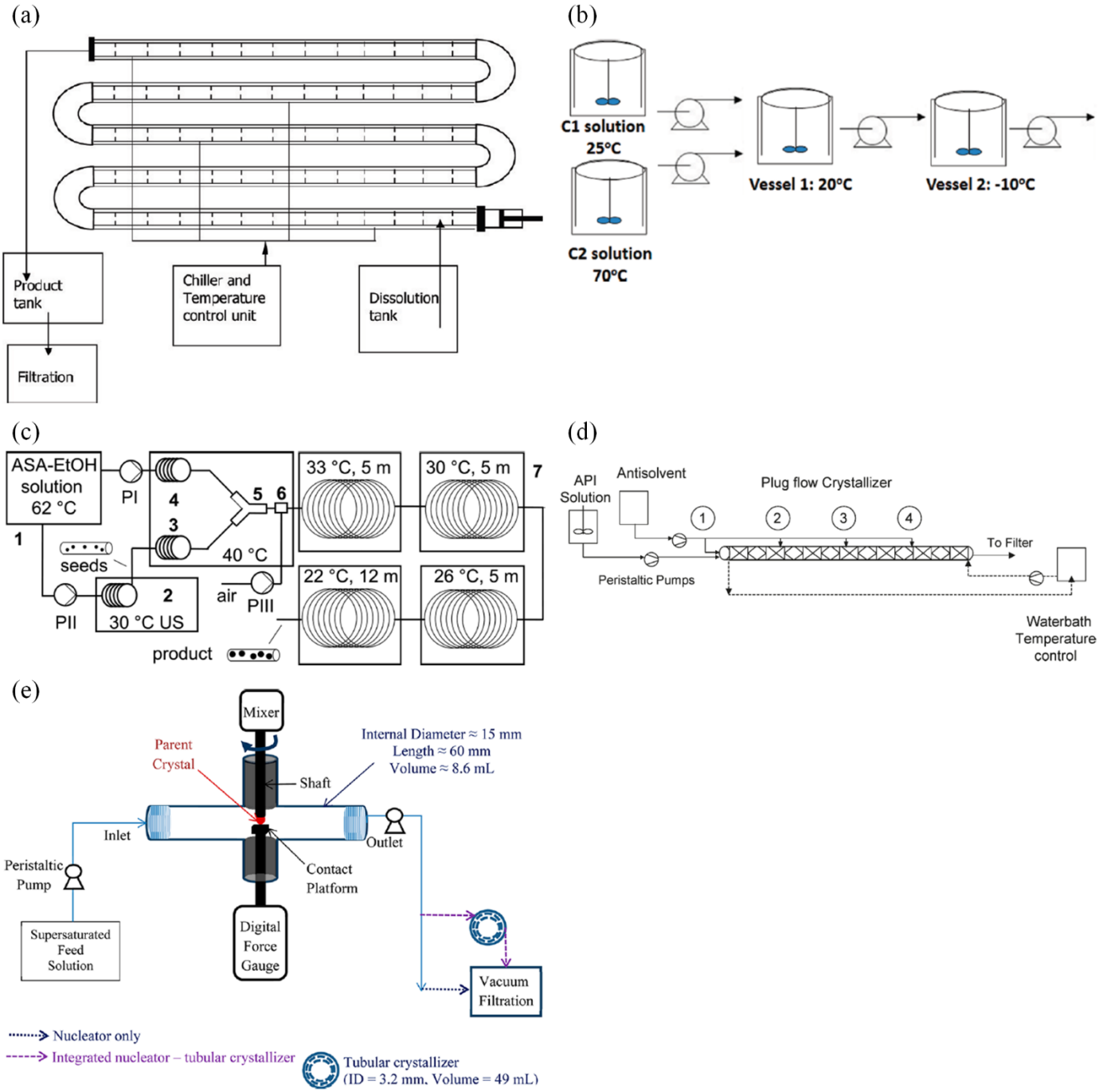

Figure 1.1. Examples of different platforms for continuous crystallisation of pharmaceutical compounds. Reprinted with permission from: (a) Continuous oscillatory flow reactor [16], (b) MSMPR cascade [33], (c) A seeded segmented tubular flow reactor [28], (d) Kenics static mixer with multiple anti-solvent addition [27] and (e) Tubular crystalliser with contact secondary nucleation device [34]. Copyright American Chemical Society.

1.2 Principles of Crystallisation

1.2.1 Supersaturation

This section provides a general overview of key principles and modes of crystallisation relevant to continuous crystallisation of pharmaceuticals. For a more comprehensive background of the fundamentals of crystallisation, the interested reader is directed to one of the many detailed and helpful texts on the subject [35-38]. There are various crystallisation approaches that can be used to achieve effective purification and isolation of solids from solution including reactive, evaporative, anti-solvent (or drown-out) and cooling. Crystallisation from melts, where solidification is achieved from molten feed(s) [39-41] is not discussed further as it has more restricted utility for thermolabile organic compounds. Whichever mode of crystallisation is employed, supersaturation must be generated to drive crystallisation and the two main processes involved, nucleation and crystal growth, both depend on supersaturation as the primary driving force.

Supersaturation can be described by the difference between the chemical potential of the solute and the value of the chemical potential at equilibrium:

$$\Delta\mu = \mu - \mu^* \qquad \textbf{Eq. 1.1}$$

where μ,is the chemical potential of the solute being crystallised and μ^* is the chemical potential of the solute at equilibrium at the same temperature and pressure. For any conditions where $\mu > \mu^*$ the solution is supersaturated and a reduction in the chemical potential through crystallisation of the solute can return the system to equilibrium, $\Delta\mu = 0$. Assuming ideal conditions, the supersaturation, *S*, can be described in terms of the concentrations of the solute by the expression:

$$lnS = ln\frac{c}{c*} = \frac{\Delta\mu}{RT} \qquad \textbf{Eq. 1.2}$$

where *R* is the gas constant (8.314 J mol^{-1} K^{-1}), *T* is the temperature (K), c is the solute concentration and c* is the equilibrium solubility. For practical use, this is often expressed in terms of the supersaturation ratio, S (Eq. 1.3) or as the relative supersaturation, σ (Eq. 1.4):

$$S = \frac{c}{c^*} \qquad \textbf{Eq. 1.3}$$

$$\sigma = \frac{(c - c^*)}{c^*} \qquad \textbf{Eq. 1.4}$$

It is therefore essential to know the equilibrium composition of the system under the relevant conditions in order to quantify supersaturation. For example, for a cooling crystallisation of a monomorphic system, a

phase diagram in the form of concentration versus temperature can be used (Figure 1.2). Based on this, the driving force for nucleation and growth under any given set of conditions can be determined, in principle providing the basis to select the process conditions that will deliver the required control over each stage of the crystallisation process. In Figure 1.2(a) the solid line shows the equilibrium saturation solubility curve, the dashed line the primary metastable zone limit and the dotted line shows the secondary nucleation metastable zone boundary demarking regions where it is possible to operate with or without nucleation. The arrows show the effect of cooling, evaporation as well as anti-solvent addition to create supersaturation. At point 1, the system is under-saturated, at point 2, the system is minimally supersaturated and would display only growth; at point 3, the system would display growth, secondary nucleation but no primary nucleation and at point 4, new crystals would form from primary nucleation. MSZW represents the metastable zone width illustrating the maximum undercooling before the system enters the labile region and primary nucleation occurs. Figure 1.2(b) gives an example cooling process trajectory through the phase diagram. In region 1, primary nucleation occurs under high supersaturation as the system crosses the MSZW boundary leading to the formation of seed crystals generating growth surface and selecting the polymorphic form. In region 2, a lower level of supersaturation is maintained to allow particles formed to grow whilst avoiding primary nucleation and minimising secondary nucleation. This scenario also illustrates the potential in a continuous operation to separate out each of the key process stages and utilise different processing units to manage the different process requirements presented for continuous nucleation (seed generation under high supersaturation) and continuous growth (low supersaturation). For example the high supersaturation levels required to achieve nucleation, may be better suited to a short residence time unit minimising the risk of encrustation, with slower, controlled growth best controlled in a longer residence time unit.

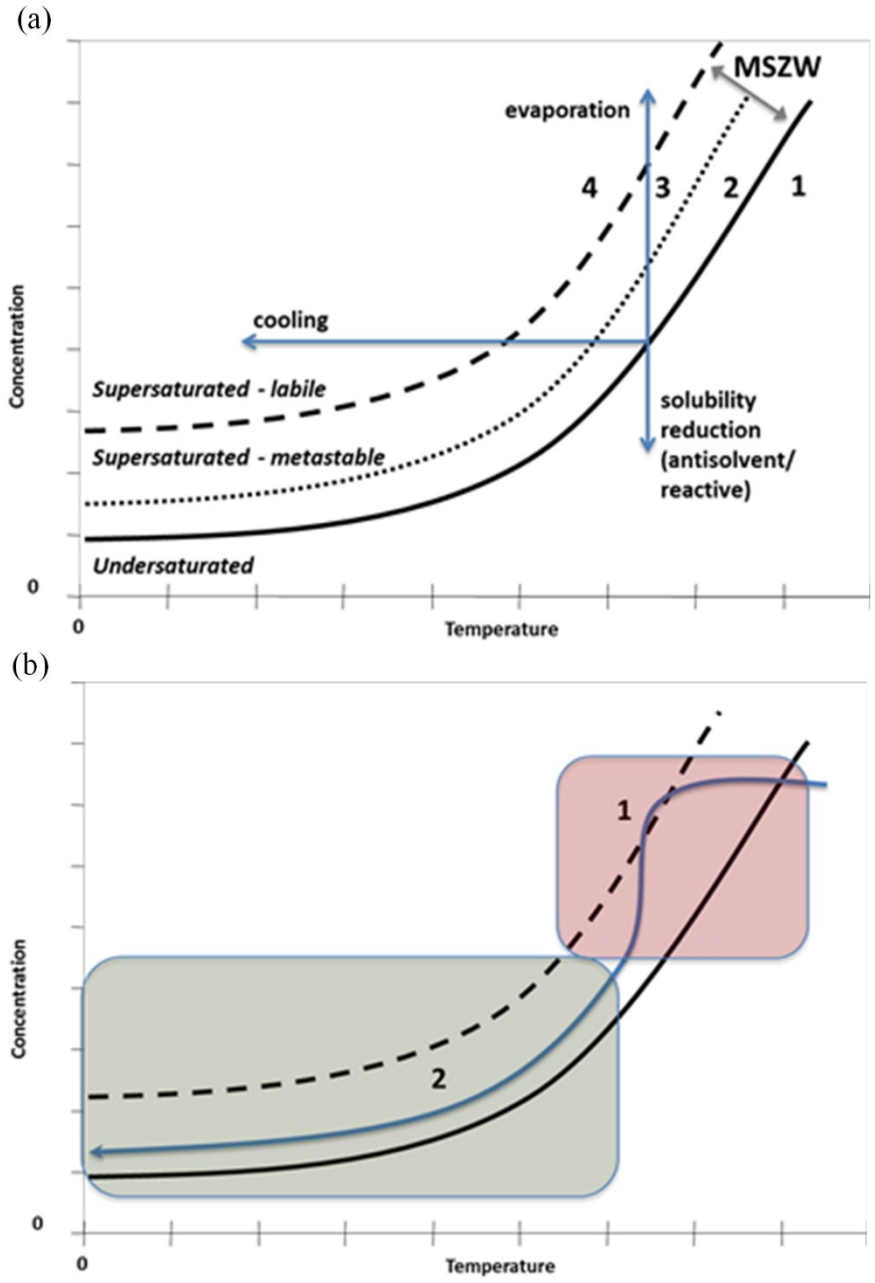

Figure 1.2. (a) General form of phase diagram for solution crystallisation. (b) Cooling process trajectory through phase diagram.

Solubility is a thermodynamic property of the system dictated by the solvent and solute and is therefore not affected by process scale or geometry. However, the metastable limits relate to the transformation kinetics and so whilst they are dependent upon the thermodynamic driving force (supersaturation) present at any given stage of the process, they are also influenced by other factors. The metastable zone width (MSZW) for primary nucleation has been shown to be highly dependent on the hydrodynamic environment within the crystalliser (geometry, stirrer type, flow) as well as on the applied cooling rate and volume and so care is required to ensure that kinetic data are collected under representative conditions.

A controlled crystallisation process involves management of the available growth surface either by primary nucleation or, more commonly by seeding, and subsequently following a trajectory within the MSZW close

to the solubility limit to facilitate controlled crystal growth whilst avoiding uncontrolled formation of new particles through nucleation. An understanding of the secondary metastable limit, where new crystals are often generated by attrition, is also valuable for processes where control of the crystal size distribution is important [42].

Anti-solvent can also be used to generate supersaturation in order to drive nucleation and growth [36, 43]. This approach may be the method of choice when the energy utilisation associated with cooling is unfeasible or when cooling alone cannot provide the necessary yield [44] and optimal yields can often be obtained by combining cooling and anti-solvent crystallisation [45, 46]. For anti-solvent addition, as with pH controlled or reactive crystallisations, consideration of rate of addition and concentration or relative addition rates of solvent or reagents requires careful consideration [47, 48]. Evaporative crystallisation generally poses challenges with control and scaling although remains a common approach in the sugar and food industry [35, 49]. Crystallisation from supercritical fluids, where the expansion of a solution is used to create supersaturation [50] can also offer specific advantages over conventional approaches but is not discussed further in this chapter.

1.2.2 Nucleation and Growth

Primary nucleation is used to describe all cases of nucleation (homogeneous [36] and heterogeneous [51]) taking place in systems where no crystalline matter is present i.e. describing the initial formation of crystals within a supersaturated solution. Nucleation can broadly be broken into two categories, primary nucleation is the formation of crystals from solution with no existing solid state of the crystallising solute. In comparison, secondary nucleation is the formation of new crystals initiated by the presence of existing crystals (seeding and attrition) [52, 53]. Primary nucleation can also be broken down further into that of homogeneous and heterogeneous. Much like secondary nucleation, heterogeneous nucleation relies on the presence of a foreign interface for the formation of new crystals, but crucially this interface is different to that of the crystallising solute. Homogeneous nucleation is therefore the unassisted formation of new crystals without the presence of a foreign interface or existing crystals. It is however generally accepted that, homogenous primary nucleation i.e. nucleation in a supersaturated solution devoid of any foreign particulates, is of limited practical relevance, particularly in a manufacturing environment. Heterogeneous nucleation, in which various potential nucleation sites are present due to contaminating materials is thought to be the dominant process in most experimental conditions.

The rate at which nuclei are formed, J, i.e. the number of nuclei formed, per unit volume, per time, is largely dependent on supersaturation. Modelling and prediction of nucleation is a highly complex process not least in part due to the challenges in measuring rapid processes at the molecular scale. Table 1.2 summarises some of the empirical relationships commonly used in the literature to describe nucleation kinetics. Specific systems will display primary nucleation at varying levels of supersaturation and this physical process is

sensitive to a wide range of process conditions including temperature, agitation as well as impurity profiles. For cooling crystallisation the MSZW provides valuable information for developing the controlled operating limits for the process (Figure 1.2). Primary nucleation kinetics have also been deduced from MSZW data, early approaches by Nývlt [54] allowing extraction of a nucleation order, m and rate constant, K with varying cooling rate but these values generally have no physical significance. Sangwal outlined approaches with the assumption that critical nuclei are formed by the attachment of further molecules to a cluster under supersaturated conditions, with approaches based on classical nucleation theory (CNT) [36] and on a power-law relationship between nucleation rate, J and maximum supersaturation, $\ln S_{max}$ [55]. Kashchiev also extended Nývlt's early approach deriving an expression relating relative maximum supercooling $\Delta T_{max}/T_0$ with cooling rate [56] and Kubota demonstrated the importance of avoiding secondary nucleation when deducing accurate primary nucleation parameters [57].

Table 1.2. A number of empirical nucleation rate expressions

Nucleation	Expression	Ref.
Primary	$J = k_b S^b$	[55]
Homogeneous	$J = A\ exp\left[\frac{-16\pi\gamma^3 v^2}{3k^3T^3(\ln S)^2}\right]$	[36]
Heterogeneous	$J = k_{b\ het} exp\left[\frac{-16\pi\gamma^3 v^2 f(\psi)}{3k^3T^3(\ln(\sigma+1))^2}\right]$	[51]
Secondary	$J = k_b S^b \mu_2$	[52, 53]
	$J = k_b exp - \frac{\Delta E_G}{T} \sigma_s^b \mu_3^k$	[58]
	$J = k_b \sigma_s^b \mu_3 (L_{min})^j$	[59]

An approach for determining J from a probability distribution of induction time, t_{ind}, has also been proposed [60, 61]. The induction time is defined as the time period between establishing a supersaturated condition to the observation of nucleation. Experimentally determined cumulative probability distributions of t_{ind} at constant S based on at least 80 t_{ind} measurements allowed the determination of J by a best fit of the derived equation to the experimentally obtained distribution. Whilst more labour intensive than derivation from MSZW the approach has been shown to be more reliable [62].

From a mechanistic perspective, nucleation remains poorly understood. CNT proposes that nucleation occurs via a step wise process, whereby molecules of solute are added to a cluster until a stable critical cluster is formed (*ca.* 10^{20} molecules) [36]. The critical cluster formation can be interpreted as an activation energy barrier to the formation of crystals [63, 64]. Whilst improved experimental techniques and the application of molecular modelling methods have provided some progress towards understanding the detailed molecular interactions by which nuclei form and develop into macroscopic crystals this remains an

evolving area of science. More recent studies suggest that nucleation occurs via a two-step model where crystalline order is preceded by the separation of a dense, disordered liquid phase [65, 66] (Figure 1.3).

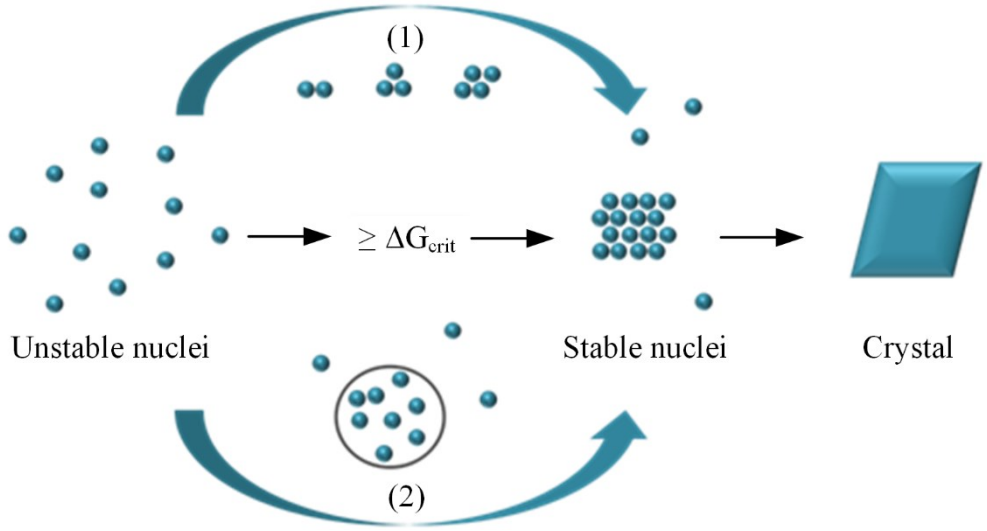

Figure 1.3. A schematic illustration of (1) Classical nucleation with growth of clusters until a thermodynamically stable critical nucleus is formed. (2) The two step nucleation process where the formation of stable crystal nuclei from disordered liquid clusters. Once critical nuclei are formed, growth will occur until a detectable crystal is achieved. Reprinted with permission from [67]. Copyright 2015 N.E.B. Briggs.

Secondary nucleation occurs when there are parent crystals present in the solution and these can induce the formation of new nuclei through several mechanisms. Crystals can impact with vessel walls, agitators, or each other and rupture depositing smaller crystals and/or nuclei into the bulk solution. A summary of the most commonly proposed mechanisms is shown below in Figure 1.4. Specifically when a narrow crystal size distribution (CSD) is a critical process attribute (CPA) secondary nucleation at different stages of the process can be a cause of significant broadening. Assessing the extent of secondary nucleation for an individual system under different process conditions is a key element of designing a controlled continuous process whether the desire is to minimise (e.g. in a PFR) or to optimise (e.g. in an MSMPR) the overall rate.

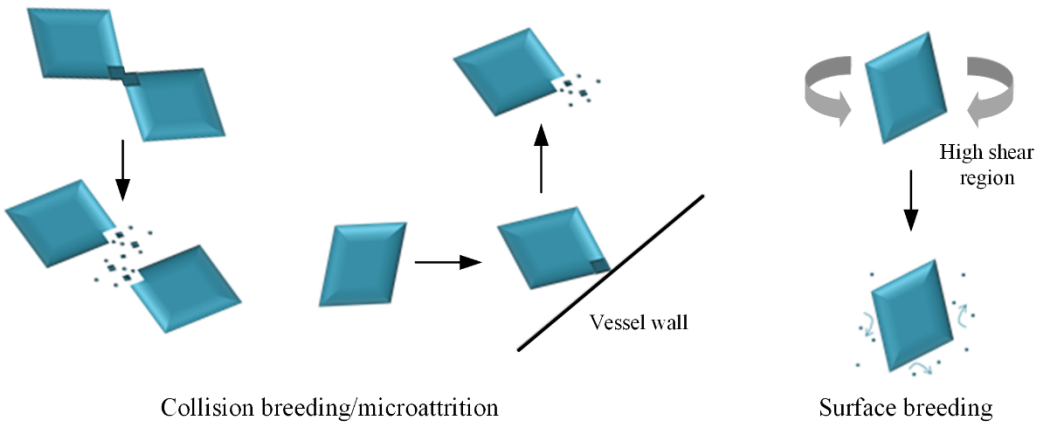

Figure 1.4. Schematic illustrating the principal mechanisms of secondary nucleation. Reprinted with permission from [67]. Copyright 2015 N.E.B. Briggs.

Once nucleation has occurred particles can continue to grow into larger, faceted, crystals and this process can be either limited by bulk diffusion or surface integration [36]. The effective growth rate is dependent on a number of factors in addition to supersaturation. These include the presence and identify of any impurities, the local mixing or hydrodynamic environment as well as attrition or particle breakage and agglomeration. Agglomeration poses one the largest challenges in interpreting crystal growth as measurement techniques such as focussed beam reflectance measurement (FBRM) and laser diffraction tend to interpret agglomerates as individual particles, leading to overestimation of actual particle size. Similarly the measurement of accurate crystal growth rates using off-line techniques such as optical microscopy may not replicate the actual process under the hydrodynamic environment of the crystalliser. A simple expression to describe crystal growth is as a linear growth rate:

$$G = \frac{dL}{dt} \qquad \textbf{Eq. 1.5}$$

Kinetic growth rate expressions can also incorporate the overall driving force and temperature effects:

$$G = A \exp\left(\frac{-E_G}{RT}\right) \Delta C^g \qquad \textbf{Eq. 1.6}$$

Where G = growth rate (m s^{-1}), L = crystal length (m), A = constant, E_G = activation energy (J mol^{-1}), g = order of overall crystal growth. A number of variations of this equation have been described to account for different types of growth kinetics (Table 1.3. Commonly used crystal growth rate expressions.Table 1.3).

Table 1.3. Commonly used crystal growth rate expressions.

Mechanism	Expression	Ref.
Size independent growth	$G = k_g S^g$	[68]
Size dependent growth	$G = k_g S^g (1 + \gamma L)^p$ $G = k_g S^g (1 + \gamma L)$	[69]
Power law growth	$G = k_g S^g L^p$	[70]

Agglomeration represents the process in which crystals adhere and grow together to form larger solid bodies [71]. The primary particles in agglomerates are generally more tightly bound than aggregates which can be redispersed easily using increased shear for example. Controlled agglomeration can however be a useful way to modify particle attributes to improve performance in downstream processes. However, uncontrolled agglomeration can lead to variability in the product PSD, difficulties in quantifying the growth of primary

particles and unexpected particle properties. For example, product can be more difficult to wash because mother liquor and impurities can become entrained inside the intergrown particles. However, larger spherical agglomerates can improve the isolation, flowability and compaction properties of crystalline products [72].

1.2.3 Conservation Equations

All of the above transformations need to be evaluated for the development of a robust and efficient process. For productivity, the conservation equations (mass, energy and population balance) will be implemented, at least in part, in industrial crystallisation unit operations. Facile calculations of crystal yield indicate only the physical mass obtained but reveal nothing on how the mass is distributed in terms of crystal sizes. Population balance equations (PBEs) account for the latter and can also include additional terms for nucleation, growth, agglomeration and breakage. Early expressions derived by Randolph and Larson [73] describe the population of crystals as a number density function n(L,t):

$$\frac{\partial n}{\partial t} + \frac{\partial (nG)}{\partial L} + \frac{n - n_0}{\tau} = B_{Ag} - D_{Ag} + B_{Br} - D_{Br} + J \qquad \textbf{Eq. 1.7}$$

L = crystal size, t = time, B and D represent birth and death terms for agglomeration and breakage, τ = residence time. Population balance modelling (PBM) can significantly reduce the number of experiments required to develop a crystallisation process and importantly the amount of material required to carry out a full design of experiments. Well-designed experiments using equipment which, as far as possible resembles the hydrodynamic environment of the process crystalliser, are essential to provide meaningful kinetic parameter estimates which can be fed into a predictive model. Many examples of the development and application of PBM for crystallisation design have been reported in the literature.

For continuous crystallisation approaches, the optimal temperature or anti-solvent addition profile must be implemented as a spatial distribution that delivers the required supersaturation or driving force at each location in the process to maintain the rate processes within acceptable, controlled ranges to achieve the required product attributes. In a continuous crystalliser the physical volume which requires to be controlled (i.e. heat and mass transfer) is significantly less than the equivalent batch reactor enabling close control. One of the important challenges then becomes managing process start-up procedure [74, 75] which allows a controlled steady state operation to be established whilst minimising waste, off-specification product.

1.3 Crystallisation Process Development

Batch crystallisations are often developed on small-scale laboratory apparatus, to establish thermodynamic parameters and applying various approaches to identify suitable cooling or anti-solvent addition regimes and seeding approaches to manipulate the crystallisation kinetics to deliver the required chemical and physical attributes and yield. This early stage work will then be scaled up to the required manufacturing scale and the

challenges of scaling up crystallisation have been well documented. There have also been a number of approaches that provide a systematic approach or workflow for the design and scale-up of crystallisations that can be applied to continuous crystallisation. However, it is also worth noting that the volume of modern potent APIs may be relatively small (e.g. < 1 tpa) raising the potential to scale process outputs based on extended operation of relatively small scale continuous platforms or numbering up processes to maintain operation under the same conditions used in development.

A workflow for crystallisation process development should support:

- A clear and systematic approach for delivery of the process with data driven decision points
- Automated data processing steps to minimise repetitive tasks
- Minimal input of operator and material resources with maximum output of data via design of experiment (DoE) approaches
- Realistic estimations of campaign timescales

Bermingham outlined a hierarchical procedure for the conceptual design of solution crystallisation processes including predictive models extracting intrinsic kinetic parameters from experimental data, as well as the analysis and optimisation tasks of the design process [76]. It was highlighted that such models could not be determined purely from first principles and limitations in analysis (e.g. determination of CSD) was an important issue in addition to physical challenges such as crystal agglomeration. Gerogiorgis presented a steady state process model and simulation for the continuous production of ibuprofen [77]. Plug flow reactors and the final purification were designed via systematic kinetic parameter estimation, solvent selection and thermodynamic property modelling. Additionally, economic and environmental factors were included. Vetter investigated the influence of uncertainty in kinetic parameters on the yield and the mean particle size obtained for crystallisation processes [78]. A methodology for uncertainty-adjusted attainable regions was demonstrated, potentially allowing the design of more robust processes. Some additional relevant studies include a generic modelling framework for batch cooling crystallisation processes [79], a practical methodology to assess the feasibility of converting batch processes into continuous [80] and a workflow for managing impurities [81].

A general framework that can be used for the development of a continuous crystallisation process are summarised in Figure 1.5. While the high level inputs required for crystallisation development are generally well known, often the underlying detail at each stage can be quite variable depending on the aims of the study, equipment used, modelling tools available and time, equipment and materials pressures. For example, choice of solvent may be restricted in a pharmaceutical crystallisation process due to environmental/economic factors or indeed based on a fixed synthetic route upstream. Some workflows may feature extensive modelling approaches requiring relevant expertise. However, this may not be available or

commercial packages may not handle unusual transformation physics. Yield may also be sacrificed for purity in some cases or downstream processing challenges may dictate residence time.

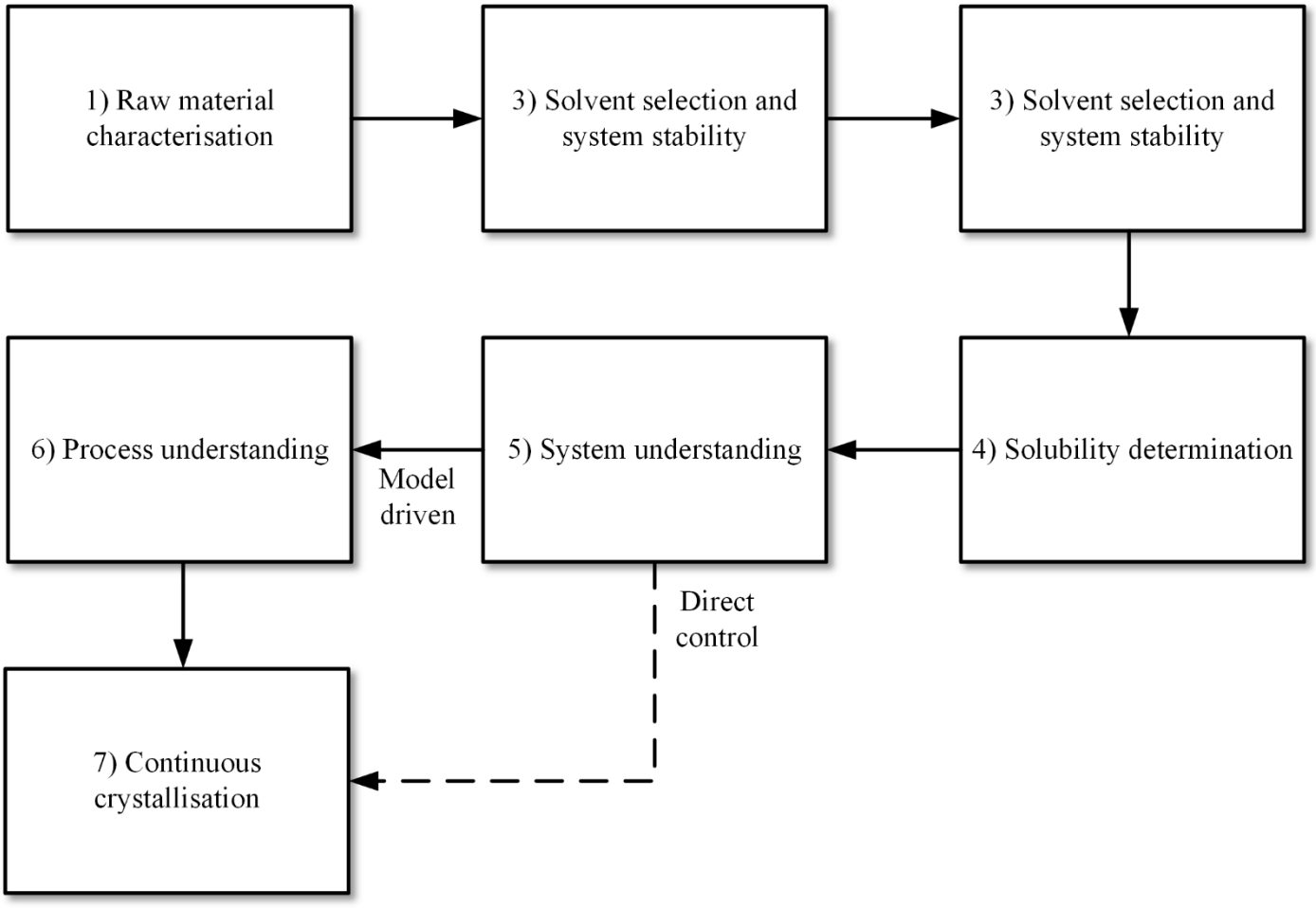

Figure 1.5. Schematic highlighting key stages in a crystallisation process development workflow.

Characterisation of raw material will include gathering existing physicochemical data from solid-state screening, preformulation or stability trials. Whilst limited data may be available, this step provides initial insight into observed behaviour and can also highlight any associated analytical challenges which may arise. It is essential to carry out chemical characterisation (as even minor impurities can have significant effects on crystallisation) as well as complete early physical reference measurements including at least structural identification. This will be aided by access to crystal structure information and morphology. Understanding variability in raw material supply including water content or composition of solvents, or variable impurities in the crystallisation may also be required. This may be particularly important where composition may not be fixed and input material may feature variability for example based on a synthetic route. It may also be necessary to develop analytical methods to quantify varying levels of impurities.

Where solvent choice is not fixed, as in a recrystallisation, then solvent screening and selection can be influenced by a number of factors (stages 2 and 3, Figure 1.5). In a manufacturing environment the choice of solvent will often be limited according to safety, cost, environmental impact or ease of disposal.

International Conference for Harmonisation (ICH) guidelines categorise solvents in three classes: 1, known to cause unacceptable toxicities; 2, associated with less severe toxicity and 3, less toxic solvents which should ideally be used where practical [82]. However, selection of a good solvent system can help to provide a robust process. In the absence of prior solubility data, a solvent screen allows a first pass at identifying solvent with no, limited or good solubilising ability. These can be readily automated to include liquid and solid dosing, control of temperature and the use of turbidity or imaging to monitor crystal properties as a function of each solvent. Early observation of extreme habits or aspect ratios, fouling or agglomeration can also be helpful. Such automated, small scale experiments can be optimised for small material amounts and generate data quickly to inform subsequent selection decisions. Advances in computational approaches for solubility prediction may increasingly allow a significantly streamlined approach to solvent selection by reducing the experimental design space required to explore. These approaches can be based on fragment based methods or thermodynamic models though do not tend to include the effect of crystal form. Multi-component solvent mixtures have proved highly challenging in terms of reasonable predictability.

Final solvent selection will primarily depend on the potential recovery, achievable solid loading and throughput in addition to practical handling concerns [44]. Further considerations may be ease of removal following crystallisation, the crystal habit produced and even physical considerations such as agglomeration. If it is possible to eliminate the latter, this may be advisable as modelling of the overall process becomes less complicated. Stability study at the most extreme conditions of crystallisation (high temperature, hydrodynamic environment) can confirm solvent compatibility and suitability. Once the solvent has been selected based on estimated temperature dependence of the solubility (or solvent/anti-solvent pairs) the solubility phase diagram can be determined. Given this will be a key tool for process development, it should be measured accurately across the accessible temperature range (stage 4, Figure 1.5). Spectroscopic, in-line techniques are becoming more suitable for such tasks (Figure 1.6). However, it is important to cross validate with additional off-line measurements.

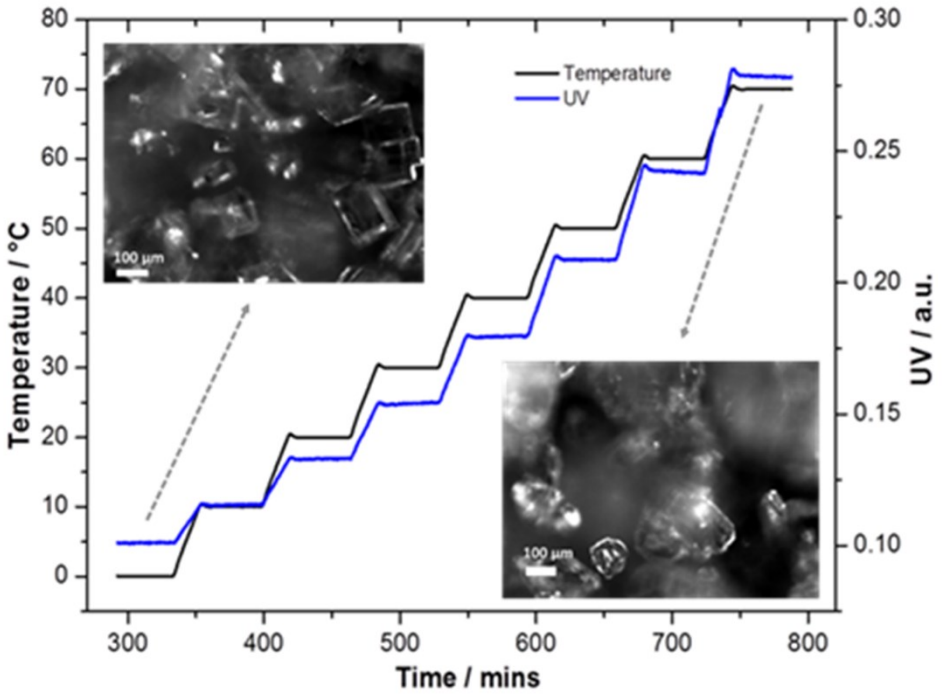

Figure 1.6. Temperature dependent solubility measurement in the presence of excess solid material using an ATR-UV method.

Whilst solubility is a thermodynamic parameter and transferrable across crystallisation platforms with varying hydrodynamic environments, the associated kinetic processes –nucleation and growth – can vary significantly, causing challenges in terms of scaling the process. Having established the solubility range of the solute-solvent system, a series of kinetic experiments can be carried out to develop further understanding of the selected system. The results provide assessment criteria for selecting of a suitable process platform. These experiments are typically batch in nature, for convenience, but should be designed to be relevant to the expected conditions in continuous equipment. Continuous platforms including microfluidics can also be utilised. An assessment of the primary nucleation limit, growth rate (Figure 1.7) and secondary nucleation rate are key aspects. However, it is also useful to consider practical aspects such as fouling propensity as function of supersaturation or with different materials of construction as this may impact on the operation of a continuous platform for extended periods. As it would be impractical to perform these kinetic studies in a continuous platform, largely in terms of material consumption, batch equivalent units, which mimic as far as possible continuous conditions can be implemented [16, 18]. To highlight this, Figure 1.8 illustrates some MSZW data collected in various platforms with different mixing mechanisms.

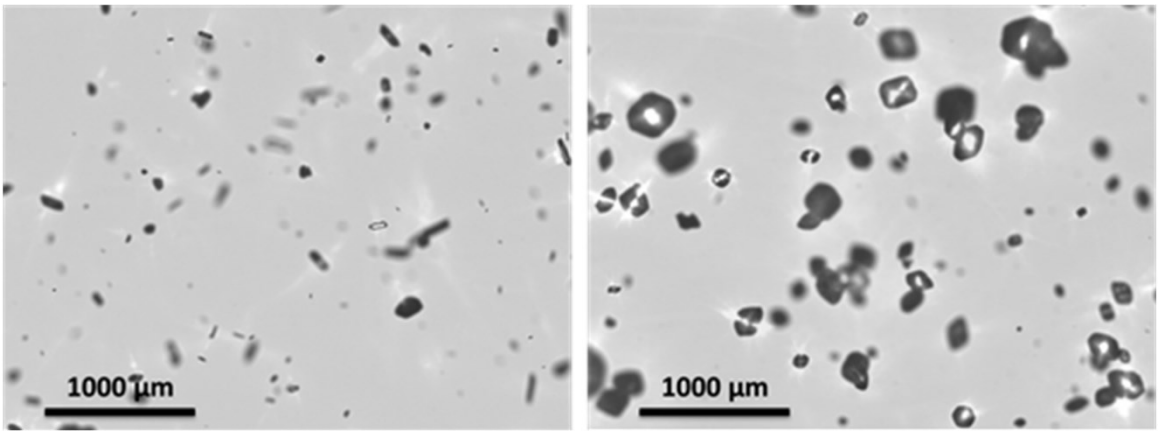

Figure 1.7. Images of crystal growth using a flow cell.

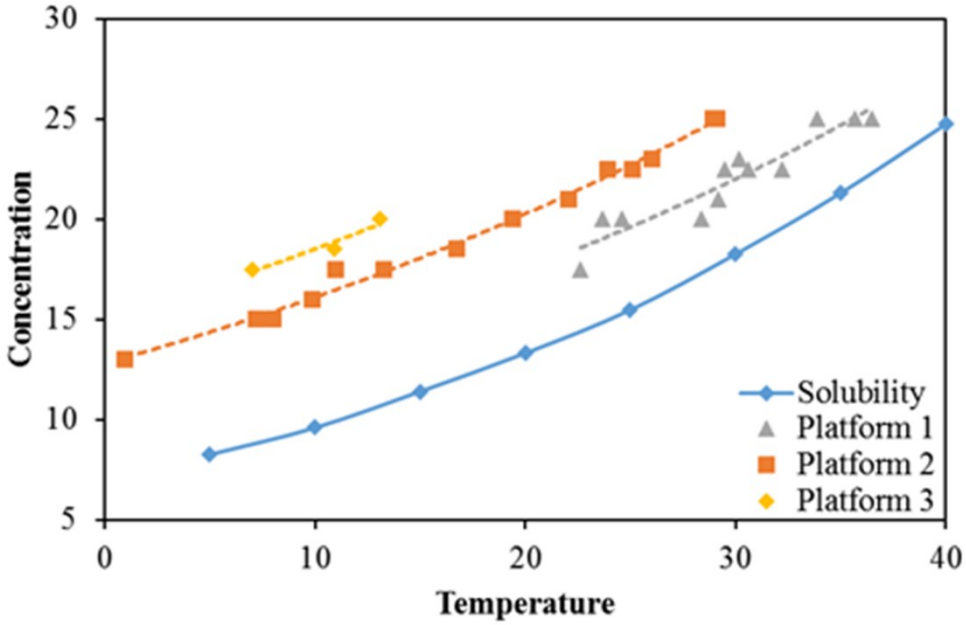

Figure 1.8. A comparison of MSZW data obtained in crystallisation parameters with different hydrodynamic environments.

Given a knowledge of the solubility limit and kinetics of the system, sensible choices about the crystallisation platform can be made based on mean residence time, solids loading and particle properties. Direct control and model predictive approaches utilising PAT could also be developed [42, 83]. In many case this may be preferred as attempting to model crystallisation processes from first principles can be extremely challenging, inherently depends on various assumptions on the rate processes and requires experience to develop, apply and validate the models. In addition real-time direct control may be able to compensate for minor disturbances during the process itself which could not be predicted in advance by a model. However, in addition to a growing number of freeware packages, commercial population balance model platforms such as gCRYSTAL [84] are increasingly allowing improved and practical approaches towards parameter estimation (stage 6, Figure 1.5) and crystallisation process model development. The potential value of these first principles models is to verify any assumptions made on the dominant processes

in the system and to allow a more predictive approach to design without the need for extensive, trial and error experimentation. For example to assess the effect of seed loading or size or of alternate temperature profiles to inform the most appropriate experiments to achieve the target product specification.

If kinetic modelling of the process using PBM has been successful and either model based or direct control approaches have been assessed, the final step is to setup and operate the continuous crystallisation process. The aim is to deliver a controlled steady state operation whilst delivering the desired purity, yield, CSD and form. This will include an efficient start-up procedure [74, 75] which minimises wastage as steady state is approached. A practical demonstration for a continuous crystallisation process should be able to operate for extended periods and deliver consistent product throughout. Practical challenges such as fouling must be effectively managed through careful control of supersaturation, clean in place or swap out approaches. Consideration for how to deal with off spec product e.g. during start-up or shut-down are also required.

1.4 Continuous Crystallisers and Applications

There are a wide variety of platforms that have been documented and described in the literature for continuous crystallisation of molecular systems including single and multistage MSMPRs, PFRs, oscillatory flow reactors (OFRs, COBRs), Taylor Couette reactors, agitated cell reactors (e.g. CoFlore^{TM}), agitated tubular reactors, segmented tubular flow systems, spinning disk reactors, impinging jets, electrospray, spray drying, extrusion systems as well as microfluidic platforms. The various crystalliser types offer different characteristics relevant to control of crystallisation processes in terms of their mixing performance, heat and mass transfer and accessible mean residence times. Many plug flow type reactors typically have shorter residence times than MSMPR crystallisers as effective mixing in the former is largely dependent on net flow. Crystallisation cycle process times to achieve complete desupersaturation can require hours and so an understanding of maximum growth rate kinetics whilst maintaining purification efficiency is required to design a robust process and inform platform selection. Supersaturation can also be controlled using anti-solvent addition, and rapid and effective mixing afforded by continuous reactors can be useful in this respect. Tubular crystallisers offer a high specific surface area and hence excellent heat transfer which enables the implementation of smoothly controlled cooling profiles, although care is required to prevent encrustation or fouling of heat exchange surfaces. As in batch processes low addition rates into a continuous crystalliser, akin to gradual or dropwise additions in batch e.g., for pH change or for anti-solvent, need to be managed carefully though can be done successfully [27]. The location and rates of multiple addition points along the length of tubular reactions can be optimized and many platforms are fabricated with multiple addition port locations to allow for flexibility over controlling the supersaturation profile for individual crystallisation processes.

Where nucleation rates are relatively slow and the mixing is ideal, MSMPR crystallisers can operate at nearly constant low supersaturation, giving rise to relatively large particles. In flow type crystallisers

including tubular reactors and impinging jet crystallisers, supersaturation varies across all positions in the reactor. The optimal strategy to select should be dictated by the crystallisation process and need to control the relative nucleation and crystal growth rates in order to achieve the required PSD [19, 23, 30-32]. Detailed models of the particle sizes that can be achieved for MSMPR cascades and plug flow crystallisers are available [85]. However, further research is required to demonstrate the full range of control over particle engineering approaches for form, size distribution, crystal shape, microstructure, surface properties and purity and the optimal strategies to achieve these for all cases. In this section we will review the main operating principles of MSMPR and plug flow reactors (PFRs) and present examples of their application for continuous crystallisation processes.

1.4.1 Mixed suspension mixed product removal (MSMPR)

The mixed suspension mixed product removal (MSMPR) crystalliser is the simplest form of a continuous crystalliser and is analogous to a continuous stirred tank reactor (CSTR) or back-mixed reactor [86]. As the MSMPR is a specific implementation of a stirred tank it offers a degree of familiarity to operators when moving from a batch to continuous process as well as lower capital investment as modifications could be made to an existing facility. A simple implementation is shown schematically in Figure 1.9. A detailed explanation of the MSMPR crystalliser can be found in the works by Randolph and Larson [73].

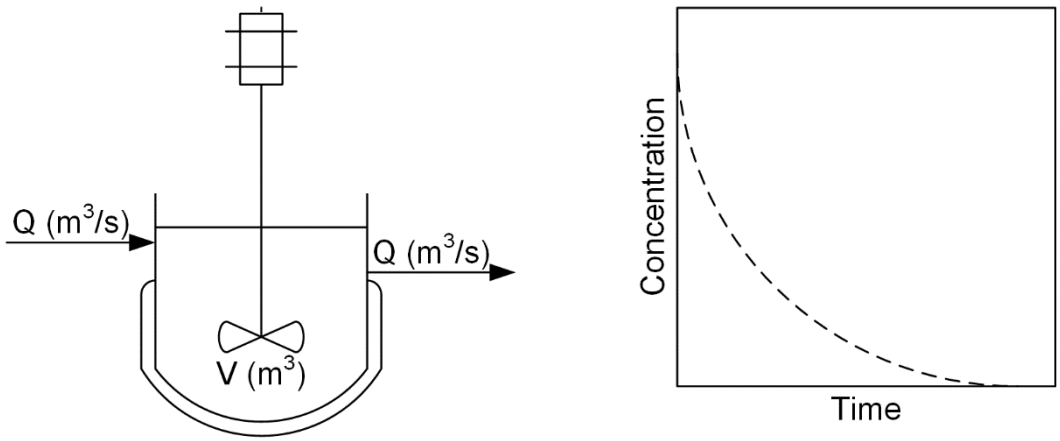

Figure 1.9. Schematic of MSMPR crystalliser and typical residence time distribution response.

Figure 1.9 shows the typical residence time distribution for a MSMPR subjected to a tracer experiment. Mean residence time, τ, can also be defined as:

$$\boldsymbol{\tau = \frac{V}{Q}} \qquad \textbf{Eq. 1.8}$$

Further discussion on the residence time distribution response of an MSMPR, readers are referred to the Tanks-In-Series model [86]. It should be noted that the inlet and outlet flow rate, Q, need not be continuous and can be intermittent [87], with the volume, V, varying between minimum and maximum levels. This periodic mode of operation is particularly suited to smaller lab scale MSMPRs where low flow rates can

lead to blockage in the outlet line. MSMPRs of course utilise stirred tanks and therefore have the advantage of utilising existing batch equipment and infrastructure to support for continuous operation with minimal adaptation. The following sections list some examples of their utilisation in continuous crystallisations.

1.4.1.1 Calcium lactate

Chemaly and co-workers [88] studied the crystallisation kinetics of calcium lactate pentahydrate in a 300 mL vessel with residence times ranging from 40 to 215 min. Each crystallisation was carried out until steady state was achieved, which was after at least 20 residence times. Crystal D_{50} size was found to initially increase with increasing residence time, before decreasing at residence times longer than 70 min (Figure 1.10). This was due to nucleation rate being controlled by supersaturation at low residence times, where as it was controlled by secondary nucleation (microabrasion) from crystal-crystal collisions at higher residence times.

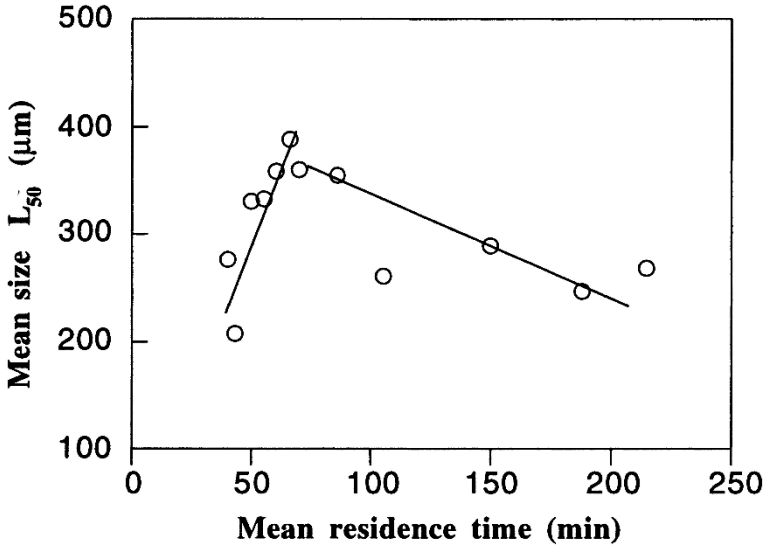

Figure 1.10. Mean particle size evolution of calcium lactate with residence time. Reprinted with permission from [88]. Copyright 1999 American Chemical Society.

1.4.1.2 Benzoic acid

Ferguson and co-workers [23] compared the anti-solvent crystallisation of benzoic acid in batch, plug flow and MSMPR configurations. The MSMPR was operated with a 375 ml volume with a mean residence time of 30 min. Steady state was observed after 7 residence times. Slurry withdrawal from the MSMPR was preformed intermittently using pneumatics. Most significantly it was found that the continuous modes of operation (MSMPR and plug flow) could obtain crystal size distributions that were both smaller and larger than the equivalent batch, in addition to delivering an increased productivity.

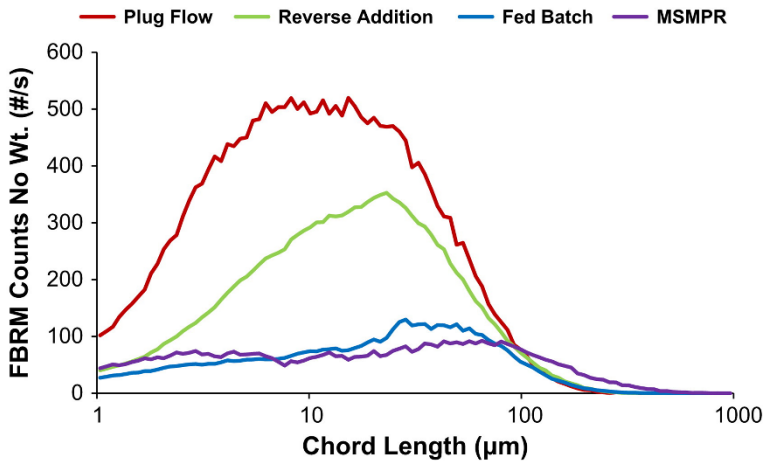

Figure 1.11. Comparison between chord length distributions from FBRM for fedbatch, reverse addition, plug flow and MSMPR crystallisations. Reprinted from [23]. Copyright 2013, with permission from Elsevier.

1.4.1.3 Deferasirox

Ferguson and co-workers [89] compared the use of their novel anti-solvent MSMPR setup (shown in Figure 1.12) to an equivalent batch process and current commercial batch process with regards to the level of 4-hydrainobenzoic acid impurity. This novel setup consisted of recycling the mother liquor from filtration back to the crystallisation to increase yield via a nanofiltration membrane to prevent that build-up of impurity (Table 1.4). The MSMPR itself was 155 ml in volume with a 1 h mean residence time and ran for 10 residence times (10 h total running). Wong and co-workers [31] also studied a combined anti-solvent and cooling crystallisation of deferasirox with recycle. In this case the MSMPR was 250 ml with a mean residence time of 1 h but with varying crystalliser temperature.

Table 1.4. Comparison of product yield and purity. Summarized from [89].

	Batch	MSMPR, no membrane	MSMPR, membrane 1	MSMPR membrane 2	Commercial batch
Yield	89.22%	70.29%	98.03%	98.71%	92%
Impurity in crystals (ppm)	0.32	0.13	0.15	0.22	0.3

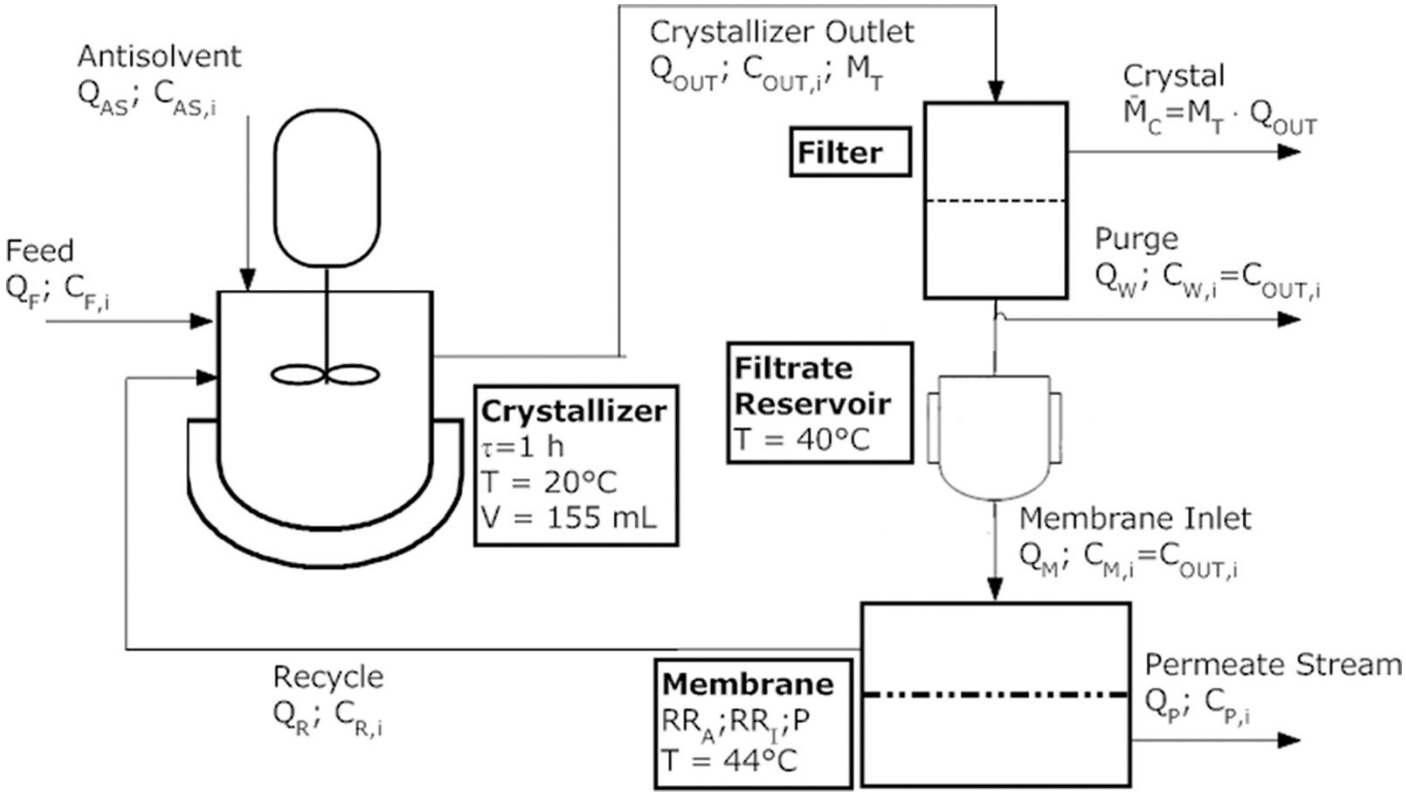

Figure 1.12. Schematic of MSMPR with recycle and integrated membrane. Reprinted with permission from [89]. Copyright 2014 American Chemical Society.

1.4.1.4 Sodium bicarbonate

Gerard and co-workers [90] studied the impact of calcium ion addition via different calcium based additives on the crystallisation of sodium bicarbonate in a 50 L MSMPR with a mean residence time of 73 min. Steady state operation was reached after 7 residence times. The identity of the additive used was shown to have a significant impact on crystal morphology, demonstrating the application of a crystal engineering approach in a continuous process to change the morphology from elongated needle to almost spheroidal (Figure 1.13).

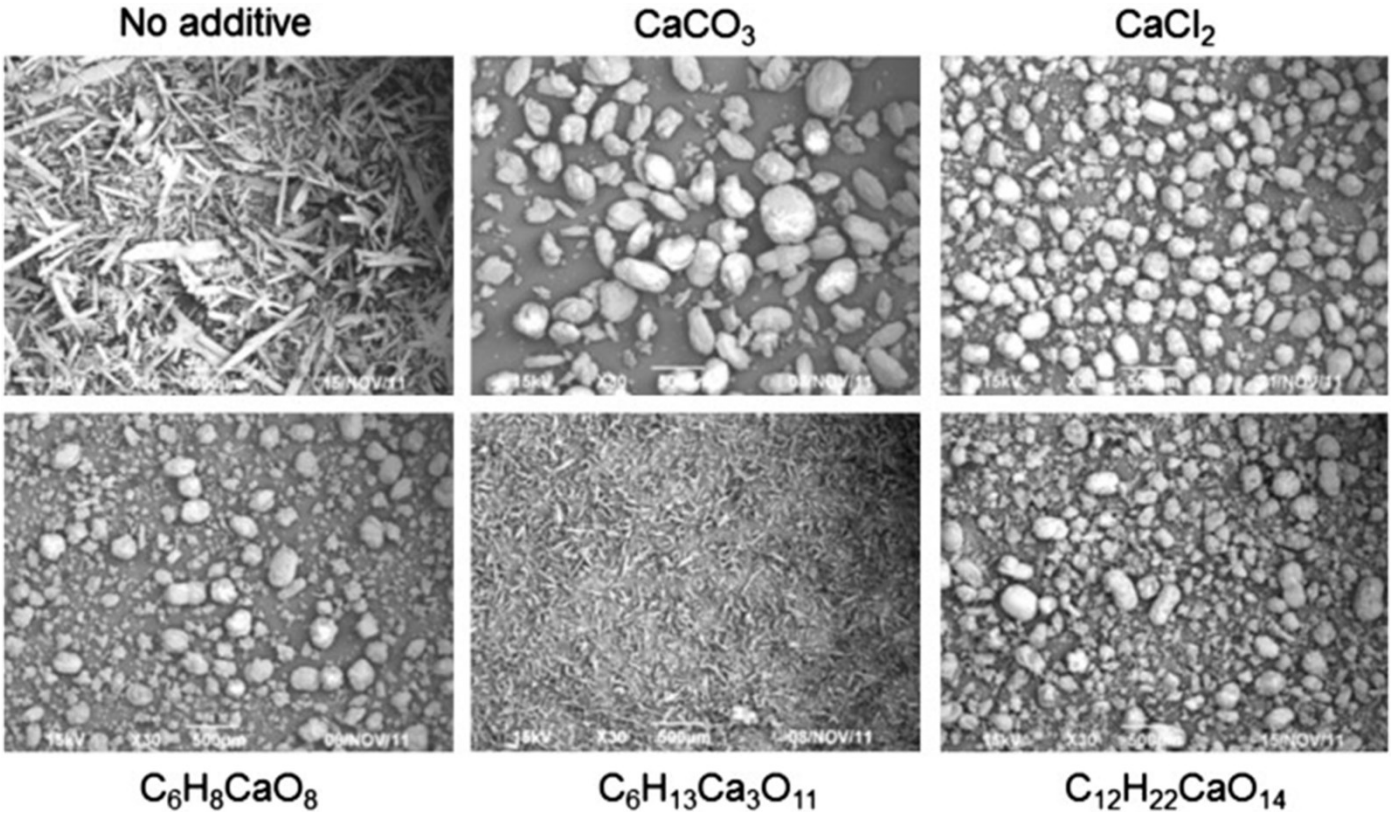

Figure 1.13. SEM photographs of NaHCO3 crystals with magnification x30 for various experiments with and without calcium based additives. Reprinted from [90]. Ccopyright 2014, with permission from Elsevier.

1.4.1.5 Paracetamol

Hou and co-workers [91] operated a continuous single stage 1 L MSMPR with intermittent withdrawal via combined pressure/vacuum. The crystallisation consisted of a cooling recrystallisation of paracetamol from an aqueous 2-propanol solution. The system was operated for over 10 residence times (τ = 40 min). This study also considered different start-up strategies finding that starting continuous operation from a seeded saturated solution obtained from a previous MSMPR run provided the quickest route to steady state operation. Yang and co-workers [92] also demonstrated the crystallisation of paracetamol in an MSMPR, but this time coupled with a wet milling unit, demonstrating the coupling of multiple operations to effect control over the process. The MSMPR was operated at 400 ml with a residence time of 20 min and operated for 12 residence times. Three configurations where evaluated: 1) without wet mill, 2) wet mill in loop around MSMPR and 3) upstream of MSMPR as a nucleation unit. Configurations 2) and 3) are shown Figure 1.14. When used upstream the wet mill was found to reduce start-up times. Additionally, using the wet mill in a loop around the MSMPR was very effective at reducing particle size and obtaining a narrow size distribution (Figure 1.15). In both configurations with the wet mill an enhancement in yield was recorded in comparison to the no wet mill configuration.

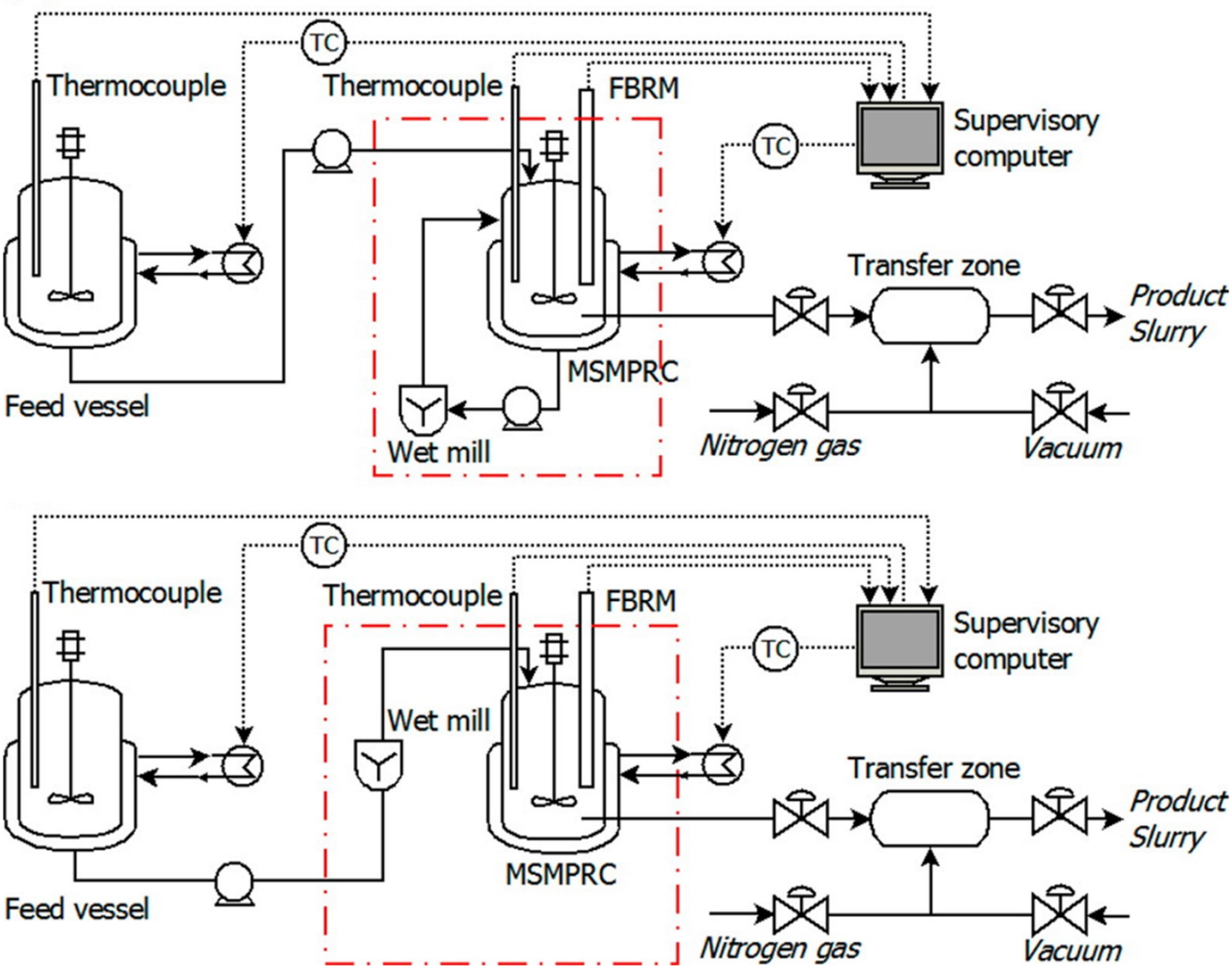

Figure 1.14. Schematic of MSMPR with wet mill as part of a loop or upstream. Reprinted with permission from [92]. Copyright 2015 American Chemical Society.

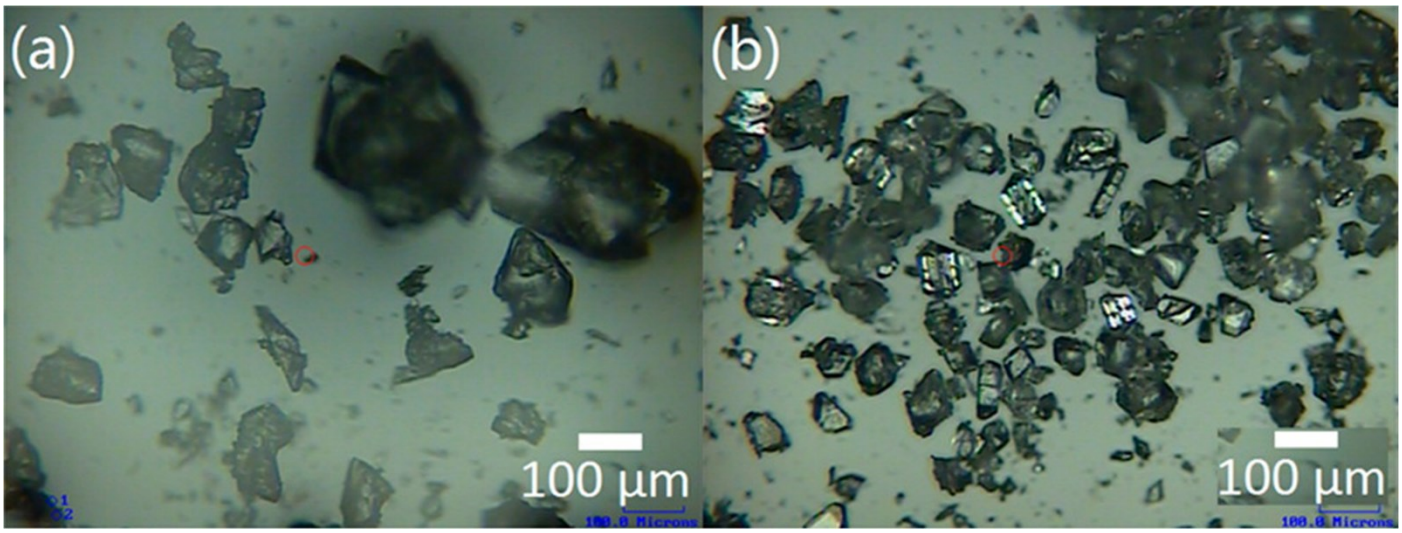

Figure 1.15. Comparison of steady state product from setup a) without and b) with met milling loop. Reprinted with permission from [92]. Copyright 2015 American Chemical Society.

1.4.1.6 Magnesium ammonium phosphate (Struvite)

Kozik and co-workers [93] performed a reactive crystallisation of struvite ($MgNH_4PO_4 \cdot 6H_2O$) in a draft tube 1.3 L MSMPR with mean residence times ranging from 15 to 60 min. Influence of pH and mean residence time of the suspension on the product size distribution and process kinetics was investigated/ Mean crystal sizes from 19 to 73 μm where obtained with coefficients of variation ranging from 60 to 87%. Providing excess magnesium ions increased the yield of struvite. However, this was at cost of the product crystal quality. Hutnik and co-workers [94] also studied the crystallisation of struvite, this time in a 600 mL draft tube.

1.4.1.7 L-Glutamic acid

Lai and co-workers [95] studied the polymorphic crystallisation of L-glutamic acid in a 150 mL MSMPR. Withdrawal from the MSMPR was intermittent, removing 10% of the slurry volume every tenth of a residence time. Residence times ranged from 30 to 120 min with a total running time up to 140 h. For unseeded crystallisations the MSMPR was first operated as a batch vessel until primary nucleation occurred, after which the feed and withdrawal systems were started. Depending on the startup conditions the initial nuclei were either pure α (25 °C) or a mixture of β and α (45 °C). Experiments with pure α during startup resulted in pure α form when operating at steady state. In comparison, those with a mixture of forms at startup produced pure β at steady state. For seeded crystallisations the MSMPR was started up with a seed mass of either pure α or β. However, the crystal form at steady state was always found to be pure α, Figure 1.16. This work concluded that operating conditions could be selected to allow for the production of either polymorphic form at steady state, but that seeding was not a valid strategy to control polymorphic form in this case, highlighting the need to consider not only the thermodynamics driving forces but also the kinetic driving forces of polymorph transformation. Tai and Shei [96] also studied the crystallisation of L-glutamic acid in a MSMPR, but focused on effect of impurities. They concluded that crystal growth and nucleation rates were suppressed by the presence of impurity. Final crystal product impurity level was also found to correlate with crystal size, supersaturation and impurity concentration in solution.

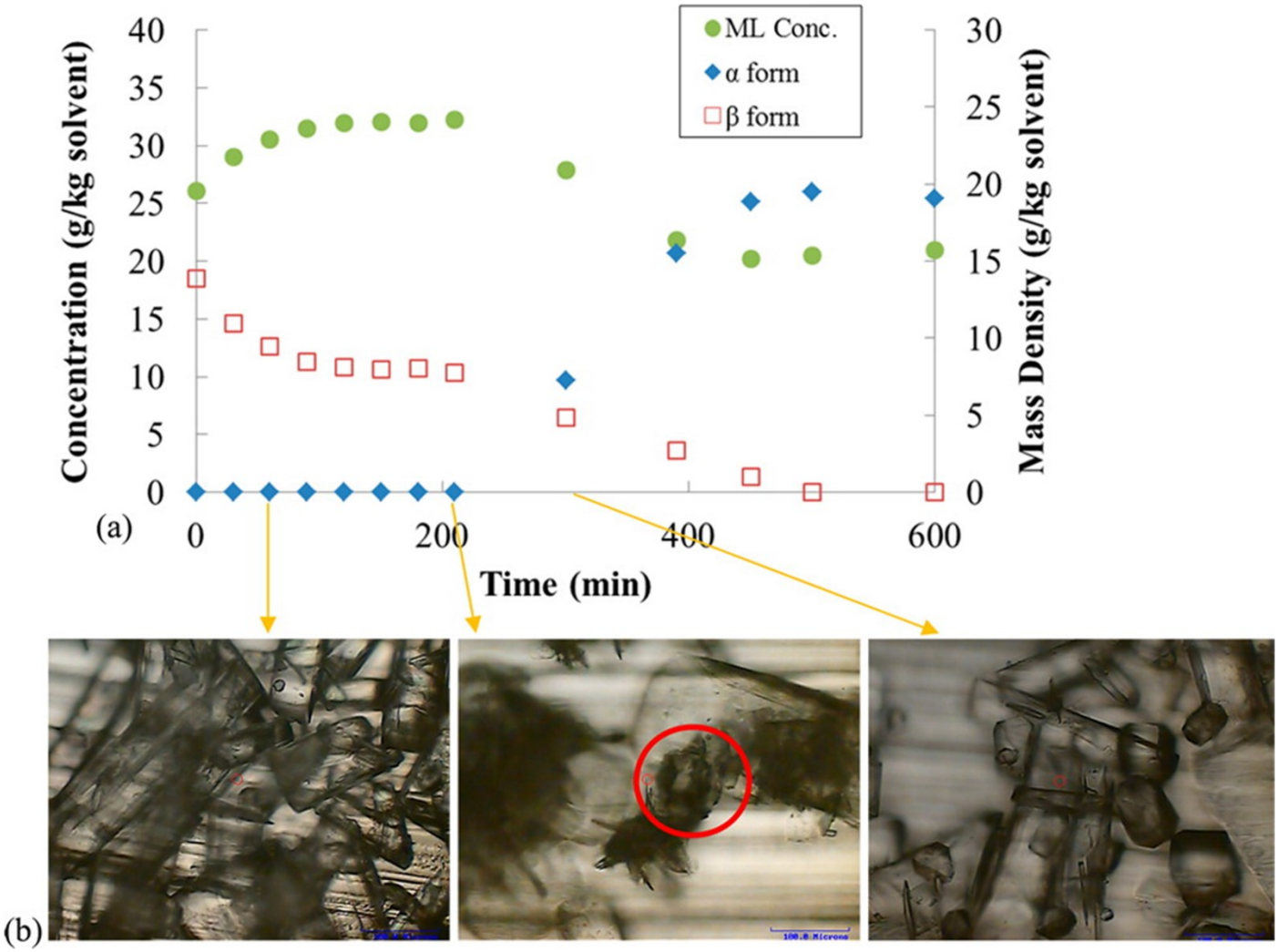

Figure 1.16. Steady state transition from β to α polymorph in seeded 25 °C MSMPR (120 min residence time): (a) polymorph mass density profiles and (b) optical images of the collected crystal samples. Reprinted with permission from [95]. Copyright 2014 American Chemical Society.

1.4.1.8 Adipic acid

Narducci and co-workers [29] also demonstrated a novel implementation of a MSMPR by coupling it with ultrasound technology. A 300 ml vessel was used as the MSMPR with residence times of 10 – 30 min. The effect of inlet solute concentration and ultrasound power amplitudes where also studied. Continuous ultrasound irradiation resulted in shortening the time required to reach steady state PSD and relative supersaturation. This lead to improved product yields. The ultrasound irradiation was also found to have a significant effect on the crystal habit and PSD (Figure 1.17), with more uniform habits and smaller sizes when compared to operation without ultrasound. In comparison to batch crystallisation a reduction in agglomeration and encrustation was also noted.

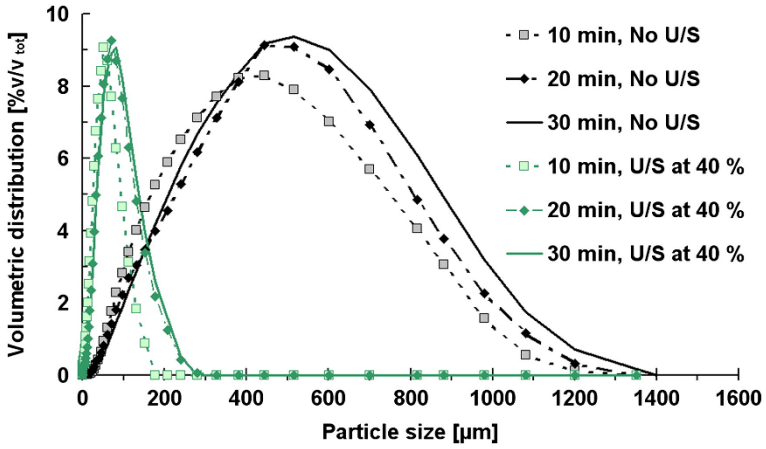

Figure 1.17. Effect of mean residence time on the crystal size distribution. Reprinted from [29]. Copyright 2011, with permission from Elsevier.

1.4.1.9 Ascorbic acid and L-sorbose

Over a series of studies Wierzbowska and co-workers investigated the crystallisation of ascorbic acid (vitamin C) in a MSMPR. Most recently [97] they demonstrated the implementation of a L(+)-ascorbic acid – ethanol – water system in a draft tube 600 ml crystalliser. At a fixed residence time of 900 s they investigated the effect of feed solution concentration leading to favourable decreases in particle size and span of particle size distribution. When studying variable residence time (900 to 3600 s) at a fixed feed solution concentration they noted an increase in solid phase at longer residence times, due to an increase in the levels of desupersaturation. Other studies included the crystallisation from methanol – water system [98, 99]. Wierzbowska and co-workers [100] also studied the crystallisation of L-sorbose in the same 600 ml MSMPR. Similar to their L(+)-ascorbic acid study they investigated the effect of feed solution concentration and residence time (900 to 3600 s) on production.

1.4.1.10 Cyclosporine

Utilizing the same MSMPR configuration as for deferasirox (250 ml volume and 1 h residence time), Wong and co-workers [31] also performed a cooling crystallisation of cyclosporine from acetone. This time the MSMPR was operated with a working volume to 155 ml with a 3 h residence time. To improve yield a recycle of mother liquor, concentrated through evaporation, was also implemented (shown in Figure 1.18). The influence of crystalliser temperature and recycle ratio was recorded on product yield and purity. Wong and co-workers also compared the performance of their setup to a multi-stage MSMPR with and without recycle and a batch processes, noting that this setup produced a higher yield of product with comparable purity and quicker start-up times (Table 1.5).

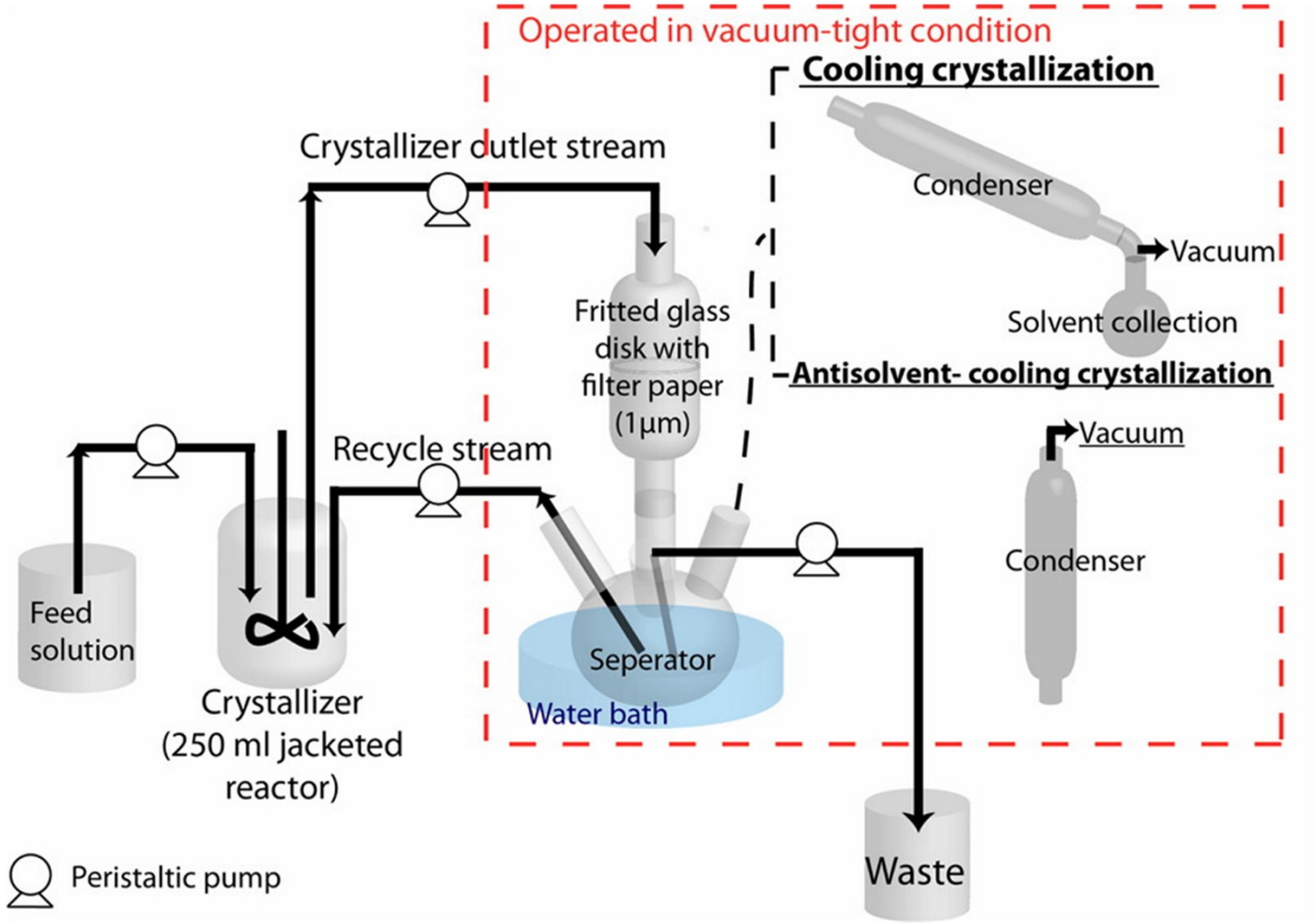

Figure 1.18. Schematic of MSMPR with recycle and evaporation separator. Reprinted with permission from [31]. Copyright 2012 American Chemical Society.

Table 1.5. Comparison of the MSMPR with recycle and 3 stage MSMPR cooling crystallisation for cyclosporine [31].

	MSMPR with recycle	3 stage MSMPR without/with recycle	Batch
Yield	91.8 %	71/87 %	74 %
Purity	94 %	96/94 %	95 %

1.4.2 MSMPR Cascade

If a single vessel, such as in the previously described MSMPR configurations, provides insufficient residence time for the crystallisation, additional vessels can be added downstream to produce a MSMPR cascade or multi-stage MSMPR. As the cascade is an extension of a single MSMPR the same benefits of a MSMPR previously discussed still apply. The potential to vary the conditions in each stage of the cascade provides additional degrees of freedom and flexibility to effect control. A simple implementation is shown schematically in Figure 1.19. A detailed explanation of the MSMPR crystalliser can be found in the works by Randolph and Larson [73] and Mullin [36].

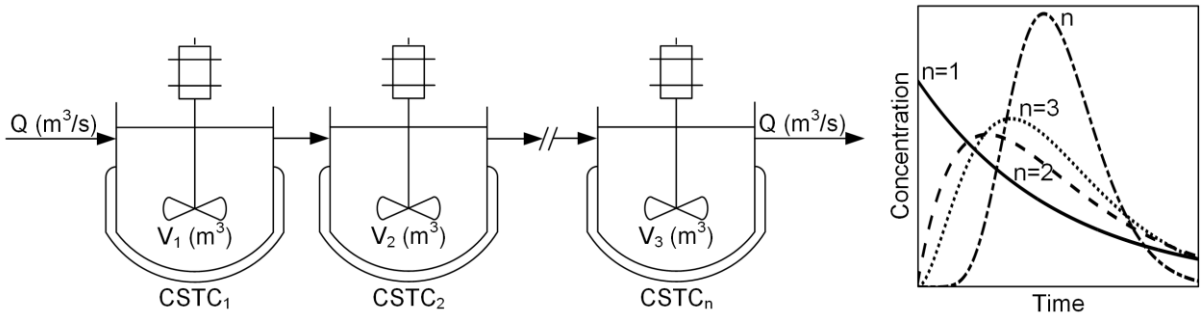

Figure 1.19. Schematic of MSMPR cascade and typical residence time distribution response.

Figure 1.19 also shows the typical residence time distributions for each MSMPR in the cascade subjected to a tracer experiment. Mean residence time can now also be defined to be based on a *per tank* or *all tank* basis [86]. As with a single stage MSMPR the inlet and outlet flow rate, Q, need not be continuous and can be intermittent [101].

1.4.2.1 Paracetamol

Power and co-workers [101] demonstrated the use of a 2 stage MSMPR crystallisation with intermittent transfer flow for the cooling crystallisation of paracetamol. The configuration consisted of two 1 L vessels, with residence times from 15 to 60 min. Steady state was also reached after 5-6 residence times. Intermittent transfer performed using positive pressure and was setup such that <10% of the crystalliser contents was transferred at any one time. Power and co-workers also highlighted the use of modelling to predict the range of product particle sizes that could be achieved for a given MSMPR configuration (Figure 1.20).

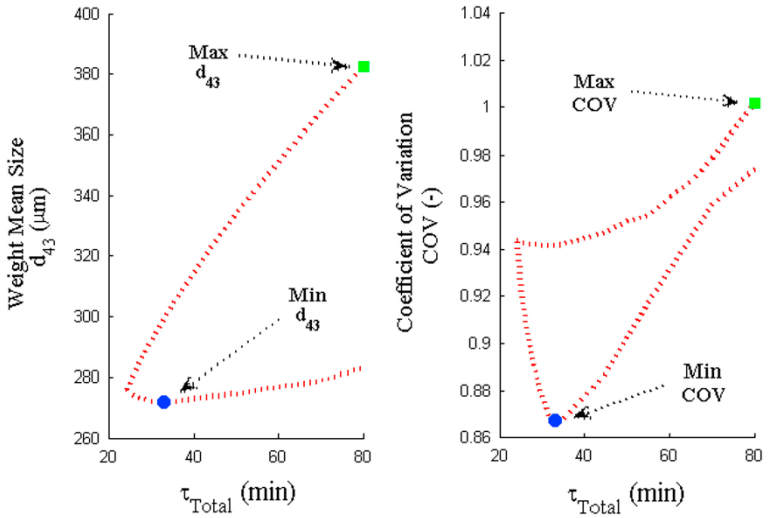

Figure 1.20. Attainable range of weight mean size and the corresponding range of coefficient of variation for the 2 stage MSMPR cascade. Reprinted from [101]. Copyright 2015, with permission from Elsevier.

1.4.2.2 Benzoic acid

Peña and Nagy [102] highlighted the use of MSMPRs for specific product attributes, in this case the spherical crystallisation of benzoic acid. This 2 stage setup offered the benefit of being able to have different conditions in each vessel, each suited for different stages of the spherical crystallisation process, in particular agitator speed and vessel volume. Residence time in the first stage was varied from 25 to 60 min and in the second stage from 45 to 100 min. Transfer between stages was via combined vacuum and pressure, transferring no more than 4.2 to 6.8% of the vessel volume. The flexibility of multiple stages allowing for different processing conditions is reflected in the range of products produced. These ranged from large spheres to small, loosely compact and flakey spheres, as shown in Figure 1.21.

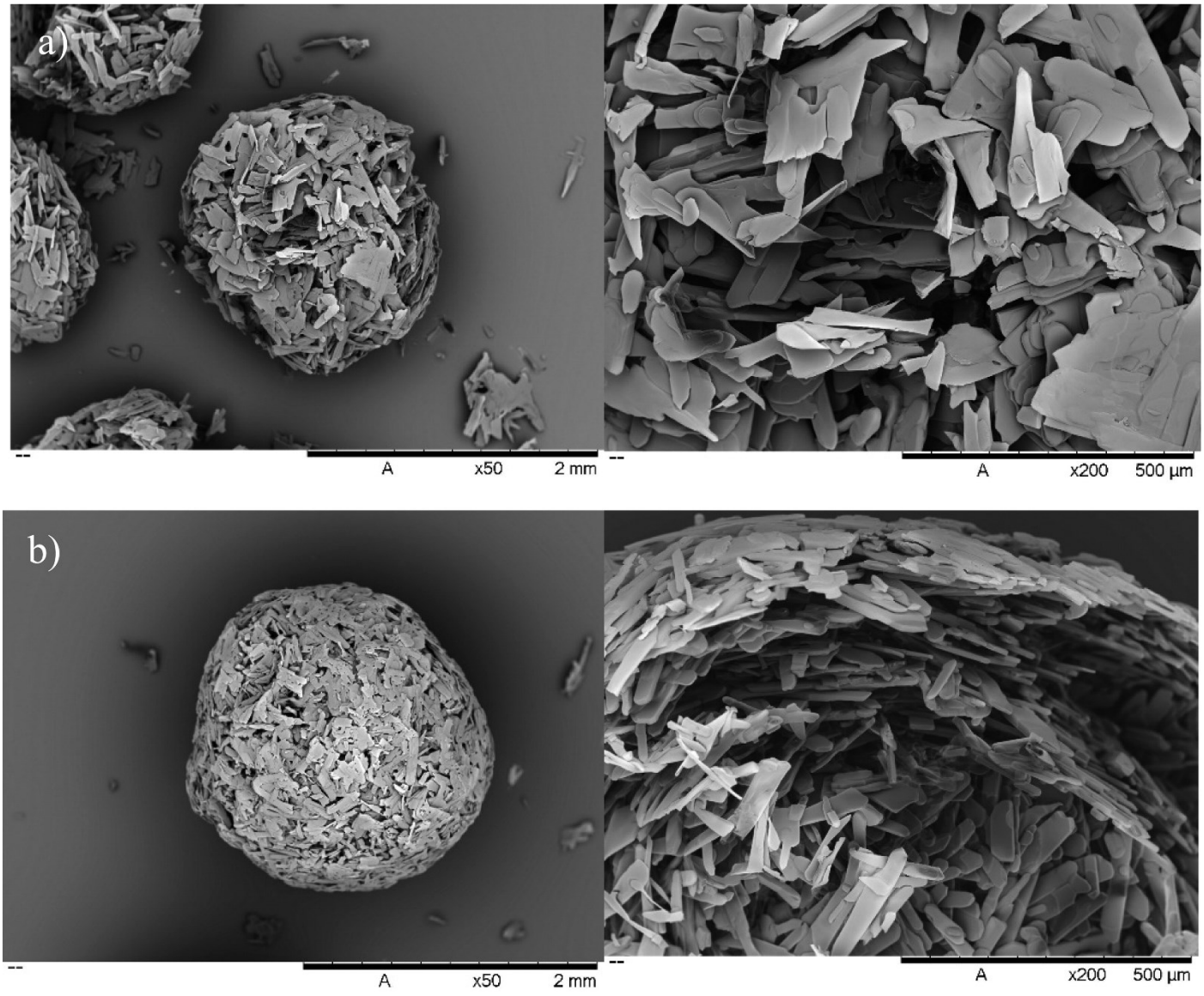

Figure 1.21. SEM images of agglomerates ranging from a) irregular shaped to b) uniform spheres. Reprinted with permission from [102]. Copyright 2015 American Chemical Society.

1.4.2.3 *p*-Aminobenzoic acid (PABA)

Lai and co-workers [21] utilized a 2 stage MSMPR cascade for the continuous crystallisation of the polymorphic compound, *p*-Aminobenzoic acid. An intermittent withdrawal scheme (10 % of vessel volume)

was implemented between the two 150 ml vessels. Residence time in each vessel was 60 min. Steady state was achieved in 2-3 residence times and the system operated for a further 4 residence time from achievement of steady state. Under steady state conditions pure α form was detected in both vessels. To investigate the stability of polymorph production, β form crystals where added to each vessel at steady state as a disturbance. Stage 1 returned to pure α form, whereas stage 2 resulted in a 75/25 % α/β mixture. Based on these experimental results, kinetic parameters were estimated for a population balance model which was used to identify the operational window for stage temperature and residence time which achieved high polymorph purity and product yield (Figure 1.22).

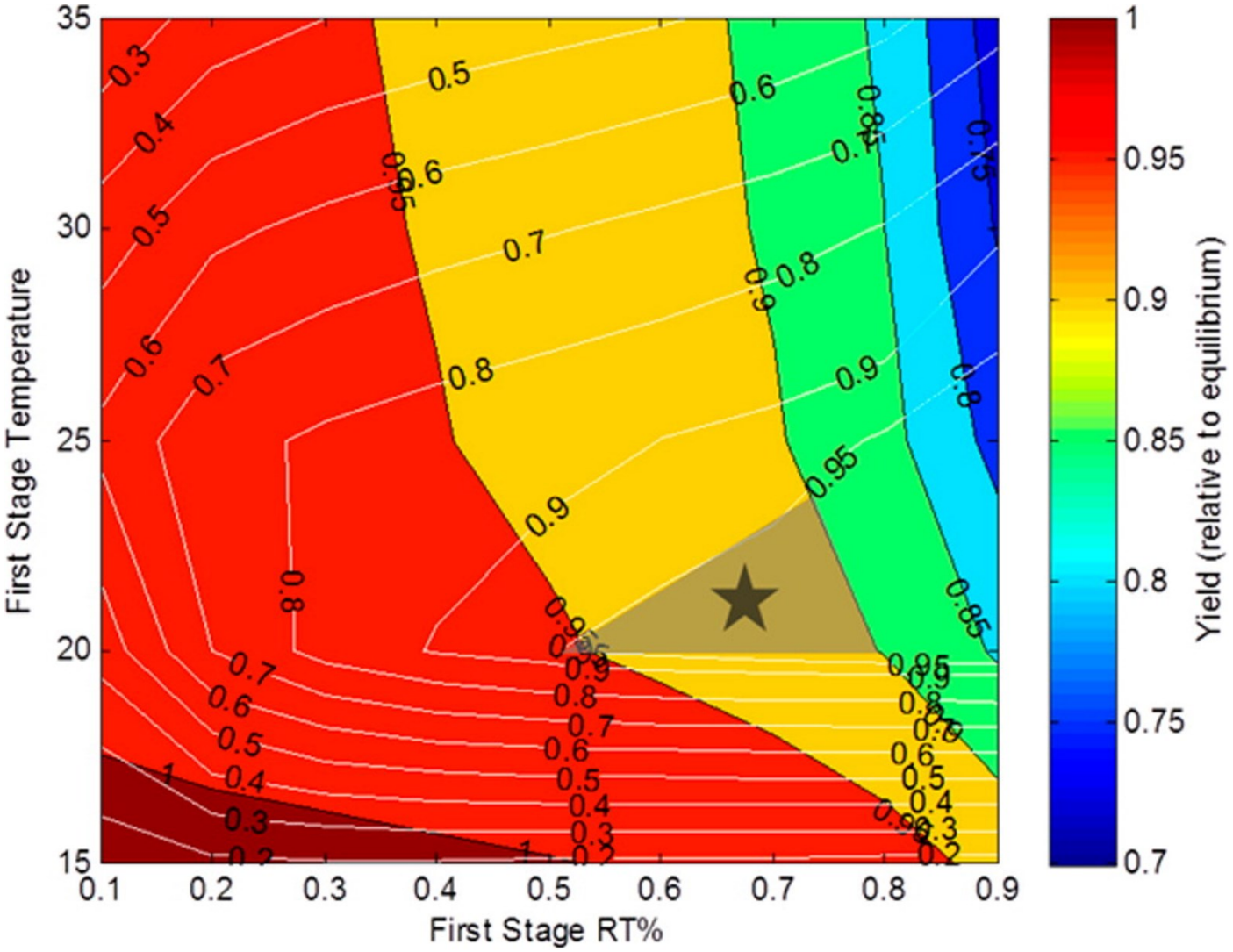

Figure 1.22. Overlapping contour plots of yield and α polymorph purity to identify the operational window. Reprinted with permission from [21]. Copyright 2015 American Chemical Society.

1.4.2.4 L/D-Threonine

Galan and co-workers [103] implemented a 2 stage MSMPR setup for the crystallisation of the enantiomeric threonine. Each vessel had a working volume of 450 ml and residence time was either 70 or 46.5 min and ran for 10 residence times to ensure achievement of steady state. The feed solution to both stages was saturated racemic mixture. To achieve preferential crystallisation each stage was seeded with a different

enantiomer. In addition continuous exchange of filtered solution was performed between stages. Slurry product from each stage was filtered and the solution recycled back to the feed vessel, shown schematically in Figure 1.23. This setup demonstrated that ability to harvest both enantiomers simultaneously at high purity is possible.

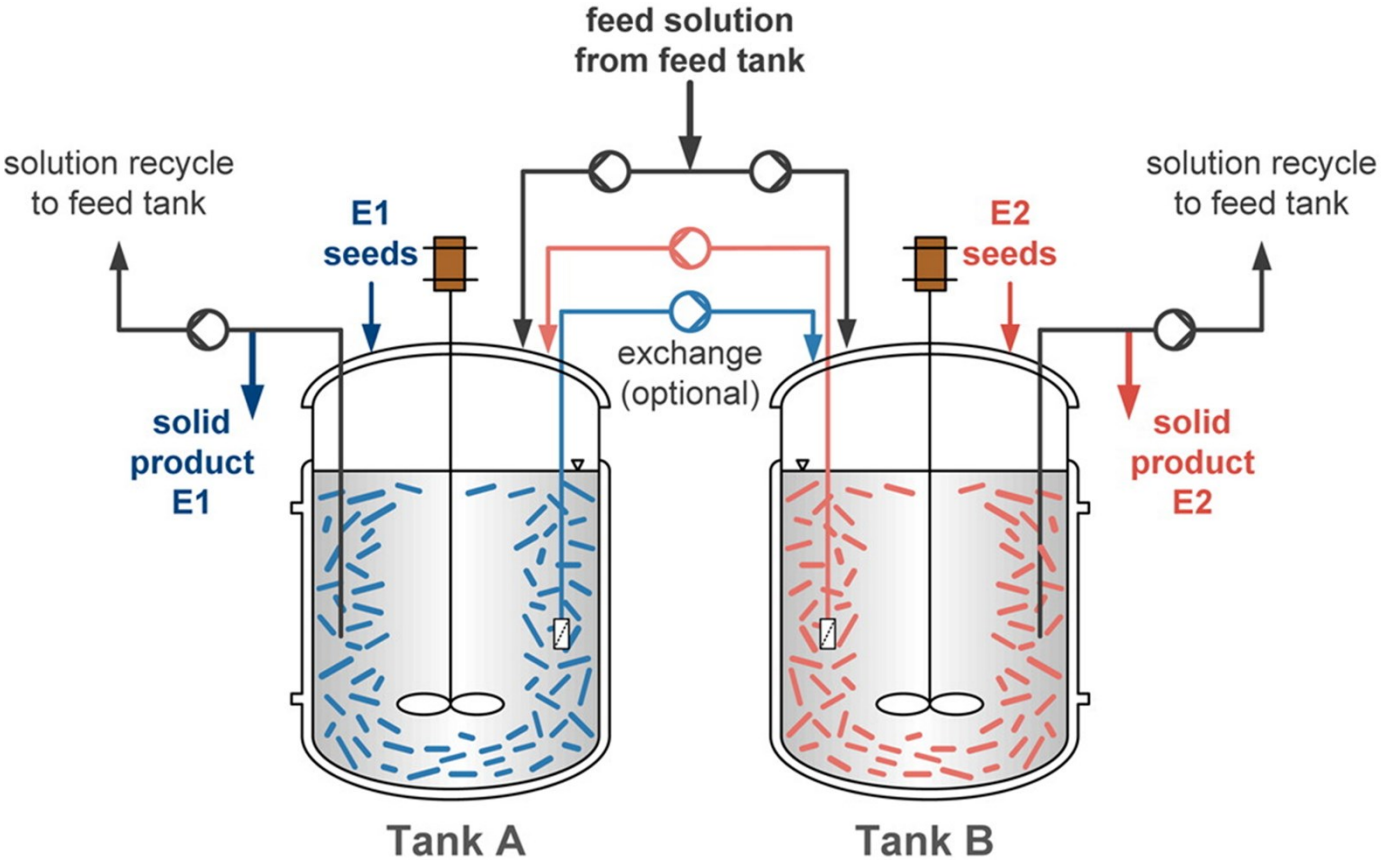

Figure 1.23. Schematic of an MSMPR cascade for preferential chiral crystallisation. Reprinted with permission from [103]. Copyright 2015 American Chemical Society.

1.4.2.5 Aliskiren hemifumarate

Quon and co-workers [33] implemented a 2 stage MSMPR cascade for the crystallisation of aliskiren hemifumarate. In this case each MSMPR stage was a 50 ml vessel operating at 20 °C and -10 °C, resulting in yields of 85 % and 92.3 %, respectively. Transfer between stages was through peristaltic pumps at a flow rate (0.17 ml/min) such that each stage had a 4 h residence time. This work also highlights a number of technical challenges when operating at this scale, predominantly the risk of clogging the transfer tubing between stages with such low flow rates. To mitigate this the pumps were operated in an intermittent manner. Operating at such low flow rates also increasing the risk of primary nucleation occurring in the transfer lines due to heat losses reducing the temperature below the saturation point. In this example transfer lines were replaced with metal ones and trace heated to maintain an appropriate temperature. Once these technical issues were overcome continuous crystallisations were run for 48 h with purities > 99 %.

1.4.2.6 Cyclosporine

Alvarex and co-workers [19] performed a cooling crystallisation of cyclosporine in a 3 stage MSMPR cascade. Each stage consisted of a 50 ml glass reactor with intermittent transfer between stages. Total residence time was 8 h 50 min and operated for 35 h 20 min (4 residence times). This study also highlighted the potential application of recycle loops to achieve increased crystallisation yields. Each of the recycle loops employed in the cyclosporine study made provision for impurity removal and/or supersaturation regeneration. Without recycle product yield and purity were found to be 71 % and 96 % respectively. Recycle of the mother liquor was also considered, which improved the yield to 87 % but at the cost of product purity, which fell to 94 %. Increasing the recycle ratio further increased the yield but with further reduction in purity.

1.4.3 Plug flow reactors (PFRs)

In contrast to the back-mixed vessels of the MSMPR and MSMPR cascade, plug flow crystallisers (analogous to plug flow reactors, see [86]) operate without significant back mixing (Figure 1.24). This can ensure that ideally every particle experiences the essentially same process conditions for a consistent residence team as it proceeds along the length of the crystalliser. As true plug flow is impossible to achieve in reality, plug flow crystallisers tend to operate with a minimal distribution of residence time, often measured by the axial dispersion, Peclet or Bodenstein numbers. Due to this very low distribution of residence time, plug flow crystallisers can generally produce narrower particle size distributions than MSMPR crystallisers. In comparison to MSMPRs or MSMPR cascades, plug flow crystallisers are typically more suited to faster crystallisers with short residence times, due to limitations on the length of reactor available. Plug flow crystallisers are not heavily in operation throughout pharmaceutical industry. This is potentially due to the high capital cost for a new installation (versus modification of an existing batch to a MSMPR setup) and the non-familiarity of the equipment to operators.

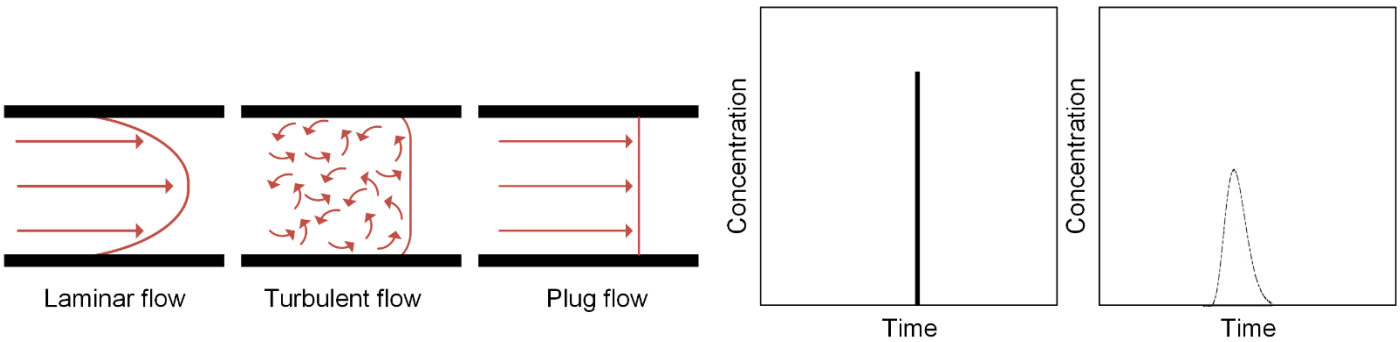

Figure 1.24. Representation of plug flow in comparison to laminar and turbulent flow. Residence time distribution response for true plug flow and typical plug flow response.

Mixing behaviour close to plug flow can be achieved through high fluid velocities in a tubular pipe. However, for the velocities typically required to achieve this the length of pipe would be unmanageable for

all but very fast crystallisations. Therefore, a secondary mechanism is usually employed for the attainment of plug flow like behaviour but at lower net velocities. These include the addition of twisted baffles as in static mixers, periodic orifices with oscillatory flow or the addition of an immiscible fluid to generate segmented flow. As plug flow crystallisers are generally tubular in geometry they exhibit a much higher surface area to volume ratio for heat transfer in comparison to stirred vessels used in MSMPR setups. This makes them particularly favourable for systems with high heats of crystallisation requiring rapid removal of excess heat. Continuous oscillatory flow reactors (COFRs) offer near plug flow where mixing is decoupled from net flow through the use of oscillatory fluid flow over baffles. This design allows longer mean residence times to be achieved in near plug flow at low residence times making them potentially well suited to slower processes such as crystallisation [16]. These crystallisers also tend to produce lower maximum shear rates compared with stirred tanks operating at similar power densities, making them suitable for suspending fragile crystals.

1.4.3.1 Lipoic acid – nicotinamide

Zhao and co-workers [104] demonstrated the use of a 25 m long, 15 mm diameter continuous oscillatory baffled crystalliser with 4.2 L volume for the crystallisation of a novel thermally stable α-lipoic acid – nicotinamide co-crystal. Continuous production allowed for the production of over 1 kg of co-crystals at a throughput of 350 g/h with a purity of 99 %. Initial control of nucleation for the co-crystal was through the addition of co-crystal seeds for the first 10 s of operation with the system subsequently self-seeding. Product crystals were large spherical agglomerates of pure co-crystalline product comprising of multiple small thin plates, Figure 1.25.

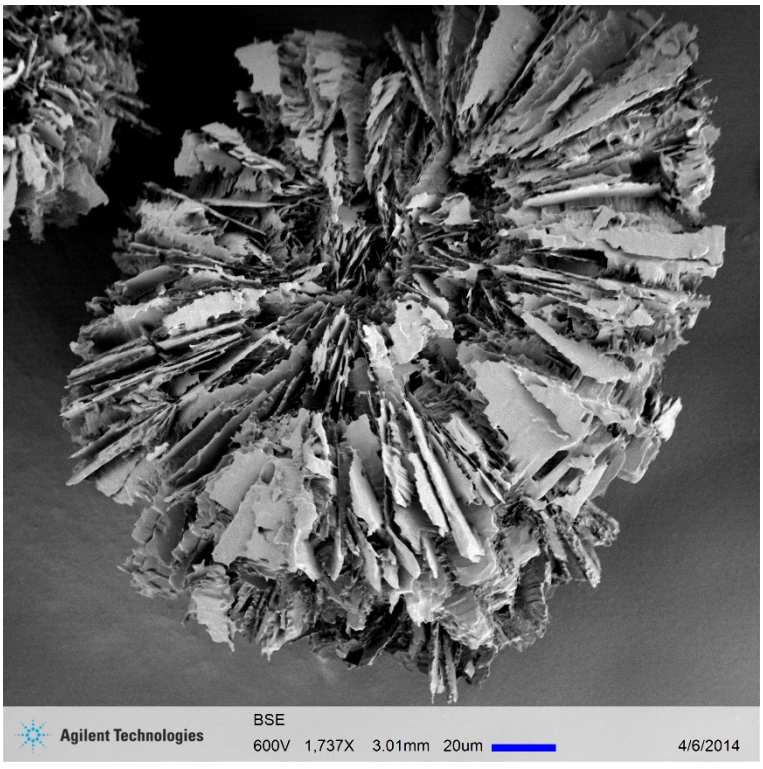

Figure 1.25. SEM images of dried lipoic acid - nicotinamide co-crystals from continuous.

1.4.3.2 Salicylic acid

Brown [105] utilized a similar 15 mm diameter oscillatory baffled crystalliser as Zhao [104] but configured to have a shorter length (1.7 m) for the anti-solvent crystallisation of salicylic acid from 2-propanol with water. Solute concentration and particle size were monitored both spatially along the length of the crystalliser as well as with operating time. With short residence times (1 to 1.5 min) to complete the crystallisation the crystalliser was operated for > 100 residence times. An extended operation of 6.25 h (250 residence times) was also performed to produce 1 kg of product crystals with a minimal variation in mean crystal size of ± 3 μm (Figure 1.26).

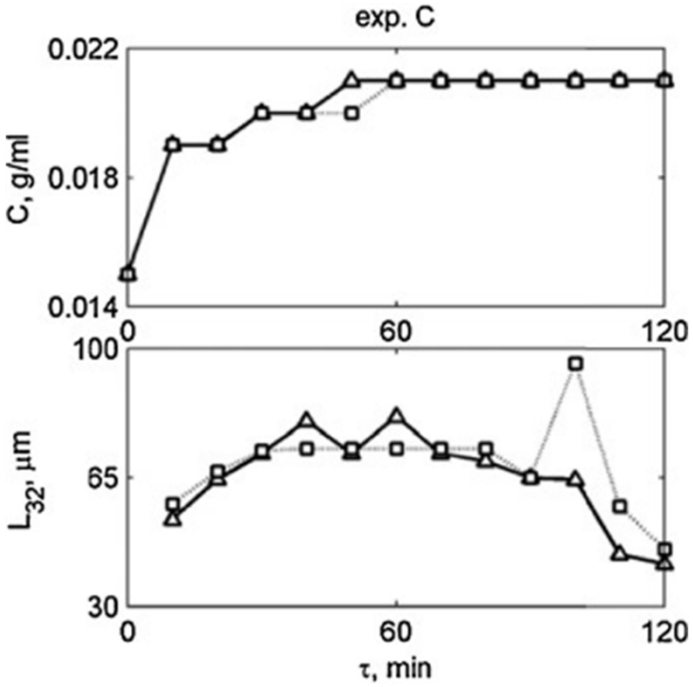

Figure 1.26. Measurements of solute concentration, C, and particle size, L, for extended operation. Reprinted from [105]. Copyright 2015, with permission from Elsevier.

1.4.3.3 Benzoic acid

In their characterisation study Ferguson and co-workers [106] employed a Roughton type vortex mixer to rapidly mix solvent and anti-solvent streams for the crystallisation of benzoic acid. The plug flow section of the crystalliser comprised of 5 m of 2.9 mm tube connected to the outlet of the Roughton mixer (Figure 1.27). Total volume was 33 ml with an approximate mean residence time of 2 s. In this study the batch and plug flow configuration were found to reach equilibrium, allowing for the maximising of yield. To illustrate the benefit of continuous crystallisers, to produce 15.8 tonnes/year of isolated product would require 43.2 10,000 L batch crystallisation versus a 33 ml plug flow crystalliser or a 9 L MSMPR crystalliser operating for 300 days per year.

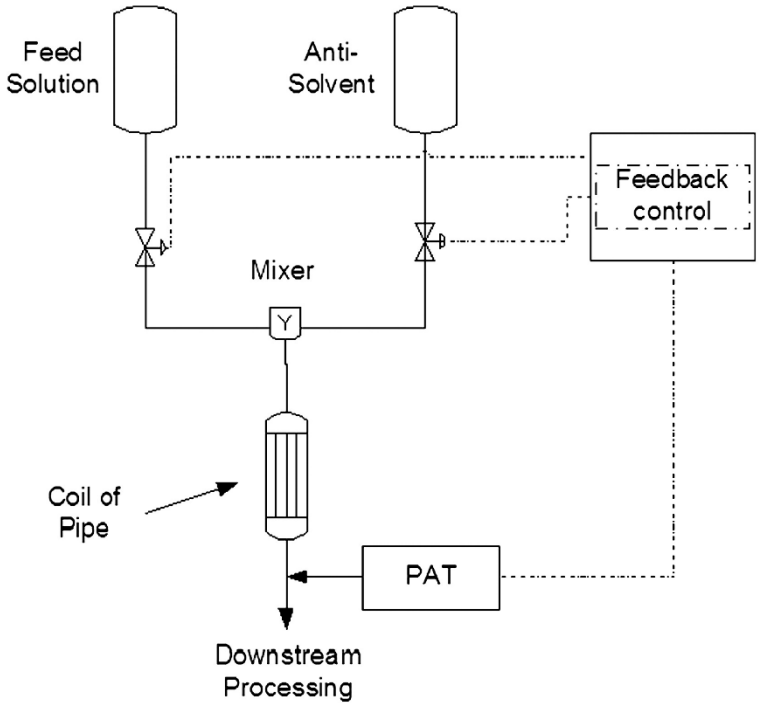

Figure 1.27. Schematic diagram of the Roughton mixer plug flow crystalliser setup. Reprinted from [106]. Copyright 2012, with permission from Elsevier.

1.4.3.4 Ketoconazole, flufenamic acid, L-glutamic Acid

Alvarez and Myerson [27] demonstrated in a series of studies the use of Kenics type static mixers, Figure 1.28, for the anti-solvent crystallisations of ketoconazole (from methanol with water), flufenamic acid (from ethanol with water) and L-glutamic acid (from water with acetone). The crystalliser consisted of up to 4 static mixer sections, each 600 mm long, 12.7 mm internal diameter with a volume of 76 ml. Solvent solution was employed as the main flow with the anti-solvent injected between each section. Number of injection points for the anti-solvent was investigated with the volume of anti-solvent split evenly between each point. Residence times studied ranged from 15 to 60 s with each experiment operating for 7 residence times. The results of this study highlighted the ability to produce small size and narrow size distributions with the capability of using multiple points along the crystalliser for anti-solvent addition to control the mean size of the crystals, Figure 1.29.

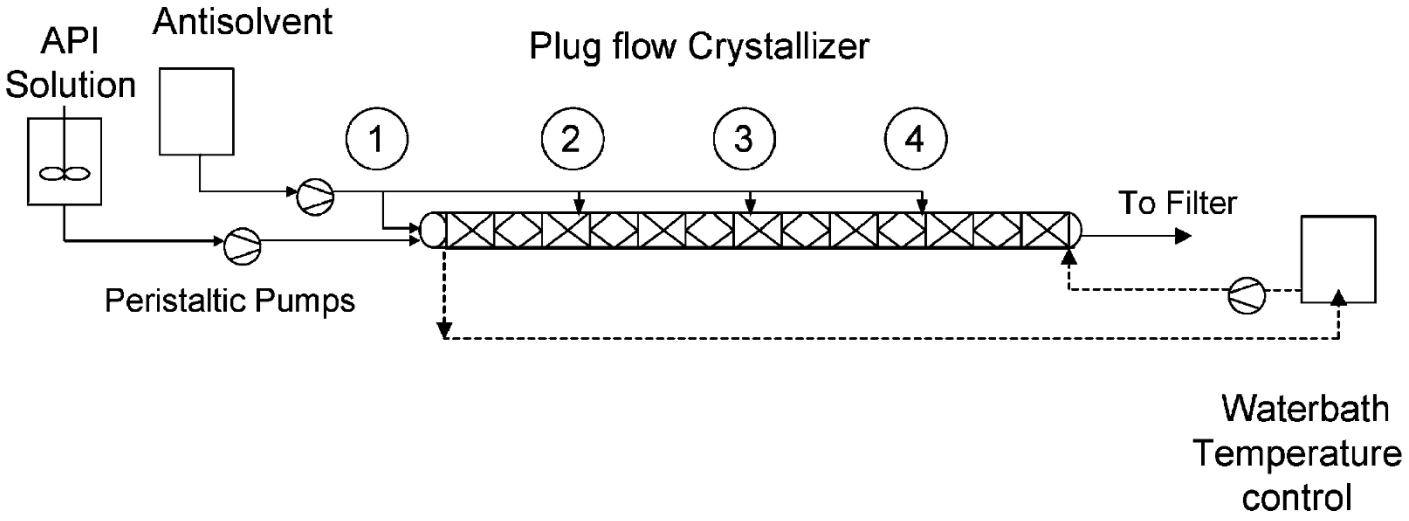

Figure 1.28. Schematic process flor diagram of the kenics continuous crystallisation system with multistage anti-solvent addition. Reprinted with permission from *[27]*. Copyright 2010 American Chemical Society.

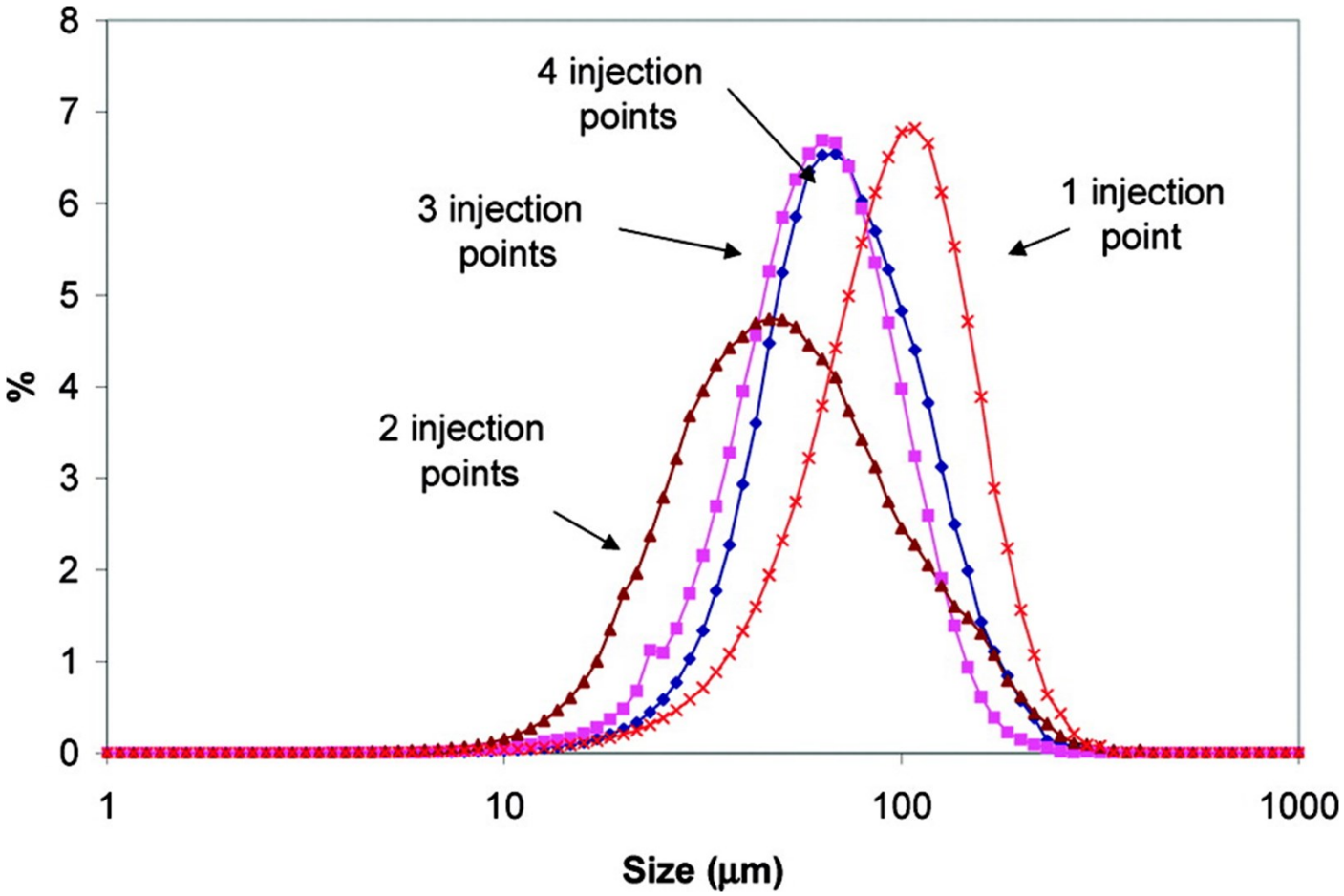

Figure 1.29. Crystal size (volume based) for L-glutamic acid as a function of the number of points of addition of anti-solvent. Reprinted with permission from *[27]*. Copyright 2010 American Chemical Society.

For L-glutamic acid, Briggs and co-workers [107] also performed seeded and unseeded cooling crystallisation in a 25 m long, 15 mm diameter continuous oscillatory baffled crystalliser with 4.2 L volume (Figure 1.30). In the unseeded experiments they highlighted one of the drawbacks of the high surface area to volume ratio tubular crystallisers in that the combination of high surface area and high supersaturation needed for primary nucleation leads to unwanted nucleation on the walls, commonly referred to as fouling or encrustation. Supplying seed crystals to the system provides a more attractive surface (the crystal faces) for growth rather than primary nucleation on the walls, leading to uninterrupted operation. For the seeded crystallisations steady state was reached by the second residence time with total operation for 8 residence times (10 h).

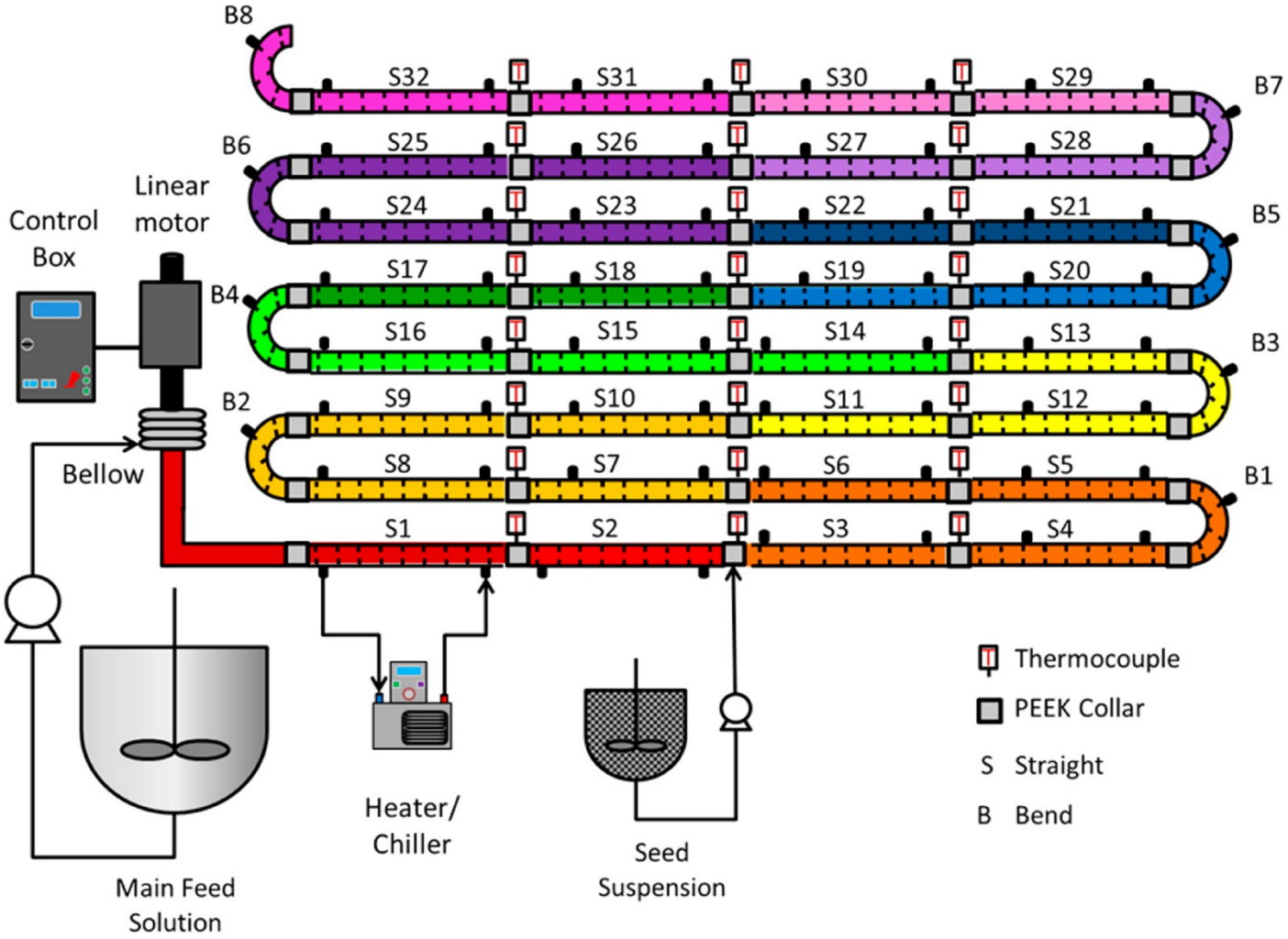

Figure 1.30. COBC setup for seeded crystallisations. Reprinted with permission from [107]. Copyright 2015 American Chemical Society.

1.4.3.5 Acetylsalicylic acid

Over a series of studies Eder and co-workers demonstrated the crystallisation of acetylsalicylic acid (aspirin) in a tubular plug flow crystalliser. Firstly, for seeded crystallisation the effect of seed crystal size and loading was investigated [108]. Solution and seed streams were mixed in a y-mixer before entering a 15 m long, 2 mm inner diameter tube to provide sufficient residence time for growth. The main conclusions were that a steady-state condition was reached rapidly, increasing seed loading resulted in decreased difference between the seed and product crystal sizes (as more individual particles were introduced), decreasing seed size whilst maintaining the same seed mass per slurry volume also resulted in a decreased difference between seed and product crystal sizes. They also highlighted the ability to adjust the temperature profile along the tube to find the optimum between sufficiently fast crystal growth, high purity, length of crystalliser and flow rate. Following on from this Eder and co-workers [28] removed the need for a secondary seed stream by applying ultrasound to a portion of the feed solution in order to induce nucleation and generate seeds in situ, Figure 1.31. In this case an additional inlet of air was produced to act as an immiscible fluid to produce a segmented flow. This combination of ultrasound and segmented flow allowed for supply of seeds of constant quantity and quality as well as minimizing the span of the residence time distribution.

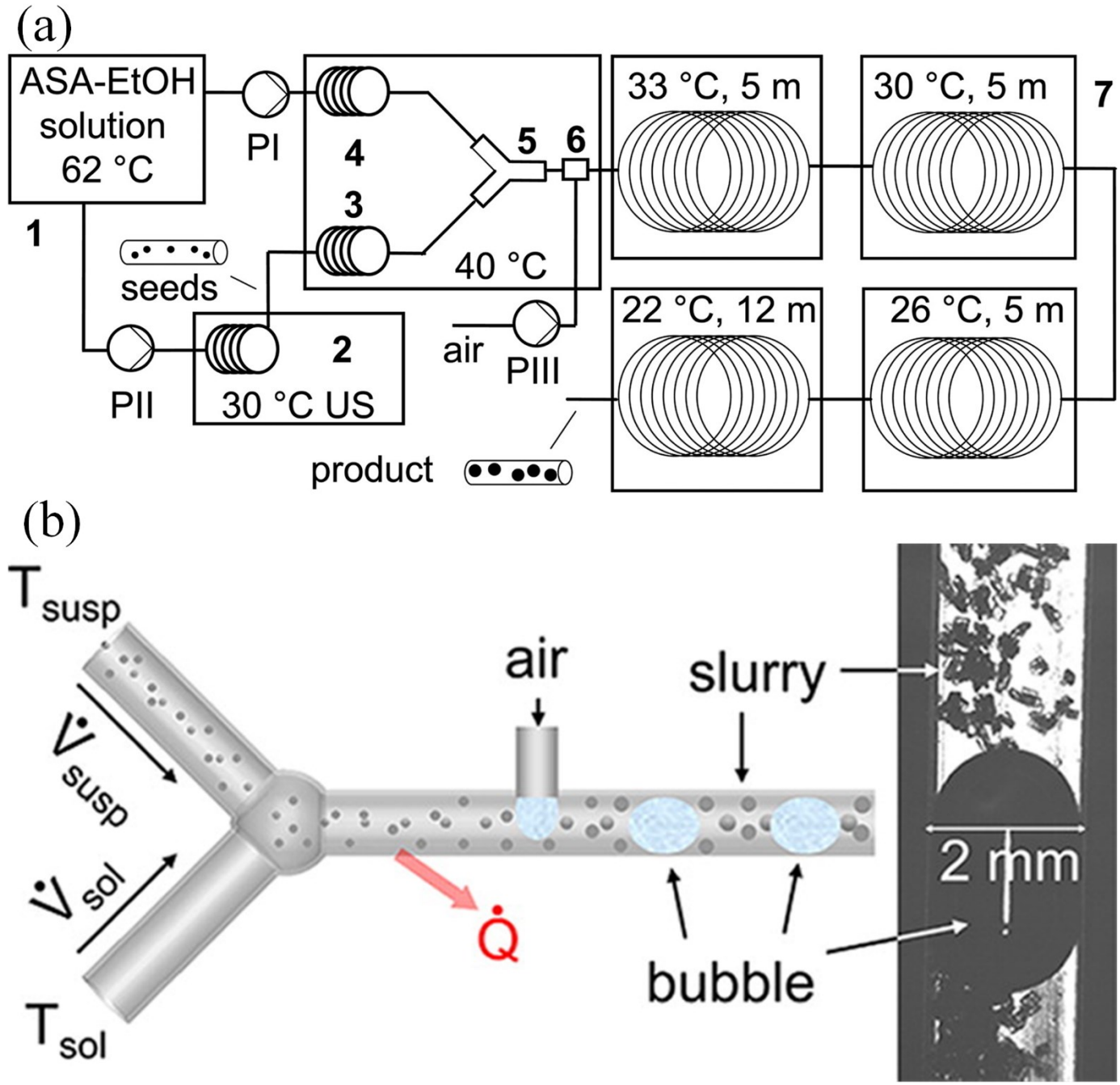

Figure 1.31. (a) Schematic of the plug flow setup with ultrasound for in situ seed generation and (b) y-mixer where solution and air are mixed to generate segmented flow. Reprinted with permission from [28]. Copyright 2012 American Chemical Society.

1.4.3.6 Lactose

Siddique and co-workers [83] also employed ultrasound in the cooling crystallisation of lactose. In this case sonication was utilized in a multi-orifice oscillatory baffled crystalliser (Figure 1.32) with residence times of up to 4 h. In this case steady state was achieved after 1.5 residence times with a total operation of 4 residence times. This study also highlighted the process intensification ability of continuous processing by reducing the cycle time from 13 to 20 h to 4 h. Narrower particle size distributions were also produced when compared to the equivalent batch process, with the ability to tailor the mean particle size through ultrasound intensity or cooling profile.

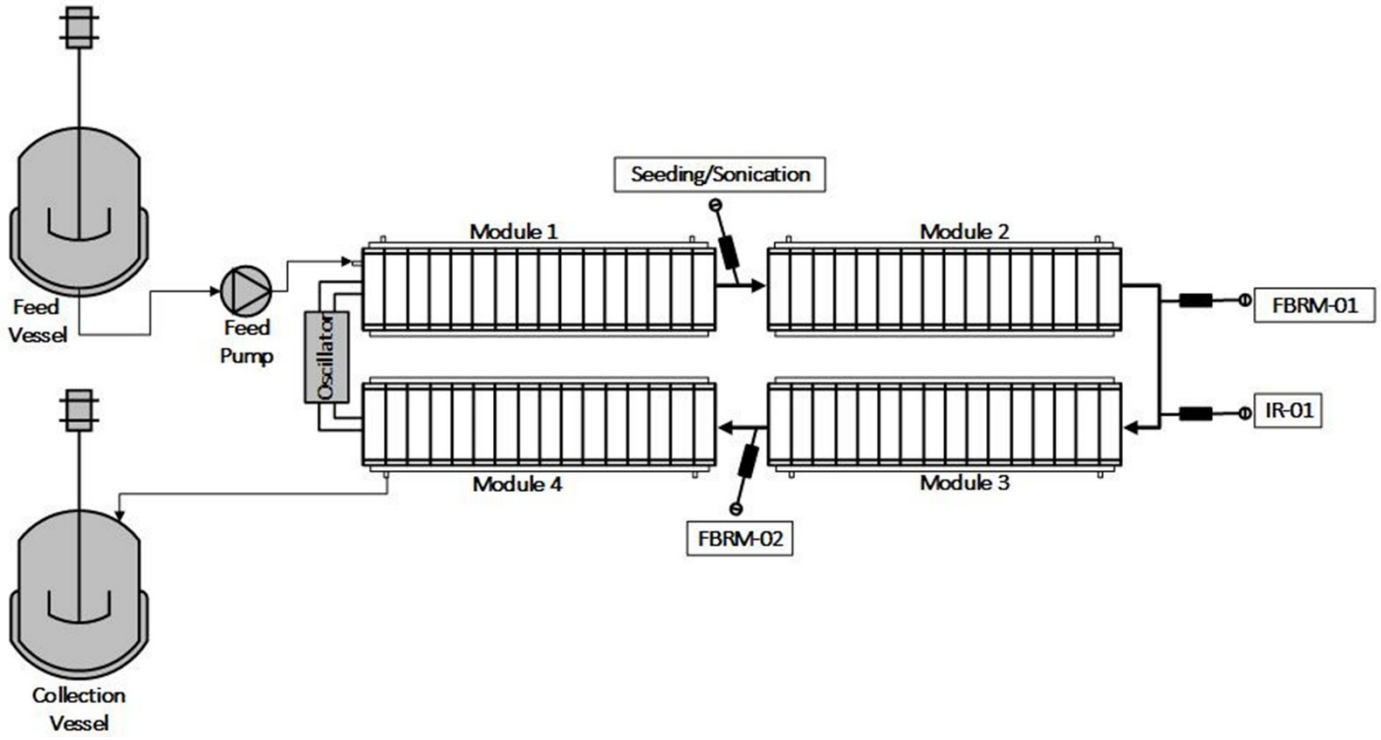

Figure 1.32. Schematic of multi-orifice oscillatory baffled crystalliser with ultrasound. Reprinted with permission from [83]. Copyright 2015 American Chemical Society.

1.4.4 Impinging jet

Similar to the Roughton mixer described previously (section 1.4.3.3), impinging jet crystallisers are a form of micromixer which can rapidly mixer two streams to generate supersaturation. Typically though solvent/anti-solvent mixing but can be combined as hot/cold streams for a cooling effect. Jet design can be either open or confined with an open geometry suitable for screening experiments as it is flexible and unlikely to clog but is subject to splashing and solvent evaporation. In comparison a confined geometry avoids evaporation, allows more control over the flow directions, allowing higher jet velocities to be reached, but does have a higher probability of clogging. Downstream of the mixer can either be a tubular section to generate plug flow, as in the Roughton mixer example, or the stream can be discharged directly into a MSMPR. Tari and co-workers [109] compared the performance of an impinging jet to cooling, reverse anti-solvent and anti-solvent combined with ultrasound processes for the crystallization of glycine. This study demonstrated the ability of impinging jets to generate very fine particle size distributions compared to traditional processes, Figure 1.33. Tari and co-workers [109] also studied the effect of jet velocity, a study which was also carried out by Jiang and co-workers [110] on an undisclosed compound. Both these studies highlighted the ability to tune the particle size distribution by varying the jet velocity.

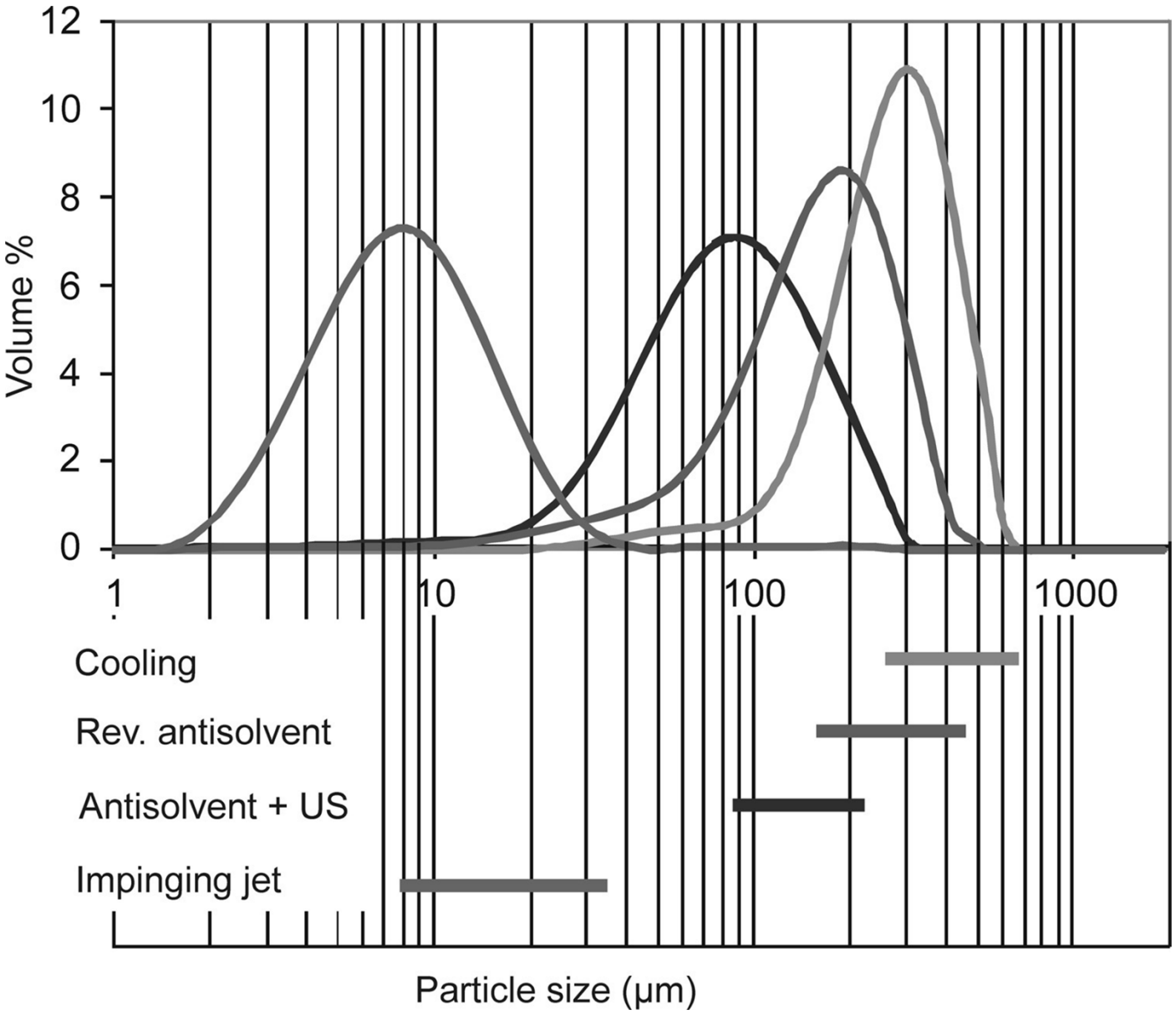

Figure 1.33. Particle size distribution and average particle size range produced by different crystallization methods. Top: particle size distribution of the product. Bottom: average particle size ranges, D(v,0.5) attained with the given method. Reprinted from [109]. Copyright 2015, with permission from Elsevier.

1.4.5 Microfluidics

Although not strictly relevant to industrial scale crystallization, microfluidic devices have been gaining popularity as a high-throughput screening tool to determine solubility, kinetic or polymorphic data [111, 112]. The most common types of microfluidic devices focus on the creation of nL to μL droplets of solution, usually separated by an immiscible fluid. This allows each droplet to be treated as an individual crystallizer. Combined with the relative ease at which droplets can be produced a wide range of conditions for crystal formation can be screened. For further information the readers are encouraged to look at the comprehensive review by Leng and Salmon [113] or details on construction from Ildefonse and co-workers [114], Goyal and co-workers [112] or Zhang and co-workers [115].

1.5 Process Monitoring, Analysis and Control

1.5.1 Process Monitoring and Analysis

Given the complex range of sub-processes associated with crystallisation (primary and secondary nucleation, crystal growth, agglomeration and attrition), developing process understanding to design and control of continuous crystallisations can be challenging and will benefit from exploiting suitable process analysis and monitoring approaches. Process analytical technology (PAT) is defined by the U.S. Food and Drug Administration (FDA) as a system of technologies for designing, analysing, and controlling manufacturing processes through measurements during processing. This has been well established in the bulk chemical industry and is becoming increasingly applied for pharmaceutical and fine chemical processes [116]. PAT have been specifically applied for crystallisation [117-119] where temperature, concentration and supersaturation can be measured in the solution phase and particle size and shape, size distribution, polymorphic composition as well as the extent of agglomeration or breakage can be measured in the solid phase using a number of different methods. The incorporation of real time (i.e. results produced within seconds) and in-line or non-invasive measurements also brings the opportunity to measure process dynamics without the risk of artefacts or misleading results due to removing and processing samples outside the reactor (Table 1.6). The introduction of a probe can effectively act as a baffle within the process stream, disrupting the fluid or slurry flow potentially creating deadzones, or may also act as a surface for fouling. In-line sampling can also be useful, e.g. combined with HPLC or UPLC methods, though care must be taken to manage temperature control, prevent particle classification to ensure representative sampling and to avoid blockage in sampling lines in the presence of particles.

Table 1.6. Summary of types of PAT implementation for continuous crystallisation.

Type of Analysis	Description	Common examples related to crystallisation
Off-line	Manual sampling, analysis elsewhere	XRPD, DSC, conventional particle sizing measurements*
At-line	Manual sampling, analysis next to process	HPLC, GC, MS*
On-line	A sample from process passes through analyser	Spectroscopic or sizing flow cell measurements
In-line	No sampling: probe inserted directly into reactor	Spectroscopic measurements, FBRM, PVM
Non-invasive	No sampling: no direct contact between sample and probe	Raman, optical imaging

* see also section 1.6

The availability and use of in-line spectroscopy techniques for crystallisation monitoring has seen rapid expansion in the last decade. In particular, attenuated total reflectance (ATR) ultraviolet (ATR-UV) [120-122], ATR-Fourier Transform mid-infrared (FTIR) [106, 123, 124] and Raman spectroscopy [125-127] approaches have all been shown to have utility. These techniques have also been implemented for operating crystallisation processes via supersaturation control (SSC) [128-132] or through direct control approaches such as direct nucleation control (DNC) [42, 133, 134] using focussed beam reflectance measurement (FBRM) and particle vision measurement (PVM). While these calibration free approaches are attractive, particularly from an industry perspective, the inherent properties of the process such as nucleation and growth kinetics are not considered, giving rise to potential vulnerability under extreme conditions (e.g. high nucleation or low growth rates) and from unexpected variations. As a result, robust calibration strategies are essential for PAT incorporation.

Table 1.7. PAT Techniques for monitoring continuous crystallisation.

Attribute to measure and control	PAT method
Solution concentration	UV, IR, Raman
Number of particles	FBRM, imaging (PVM)
Crystal form of particles	Raman
Size of particles	FBRM, imaging (PVM)
Shape of particles	FBRM, imaging

Simple univariate calibration approaches (e.g. peak height models) linking in-line spectroscopic data to supernatant concentration have associated issues such as poor reproducibility, limited ability for hardware and calibration transfer, and poor correction for external variables such as temperature, which can limit the utility of such models in terms of predictive capability. Temperature corrected calibrations are essential to control crystallisations which are performed over a wide temperature range. Correcting for spectral shifts and broadening of spectral bands as a result of temperature fluctuations [135] allows the application of process monitoring in cooling crystallisation and requires multivariate calibration approaches [136, 137]. A number of multivariate methodologies have been applied for the correction of temperature fluctuations in spectroscopic data, principally for near-infrared (NIR) measurements [138-141], where temperature is included in the calibration experimental design and modelled using piecewise direct standardization (PDS) [142, 143] and loading space standardization (LSS) [135, 144] approaches to correct for complex non-linear spectral variations. These approaches do have limitations in the range of temperature which can be corrected and can be non-trivial to develop and apply (Figure 1.34). A robust calibration approach requires identifying the concentration and temperature range of the process and gathering a representative series of spectral data to describe known compositions across this range (Figure 1.35). Having established the calibration, the measurement can then be used to quantify process responses to changes in conditions or for direct control of concentration for example.

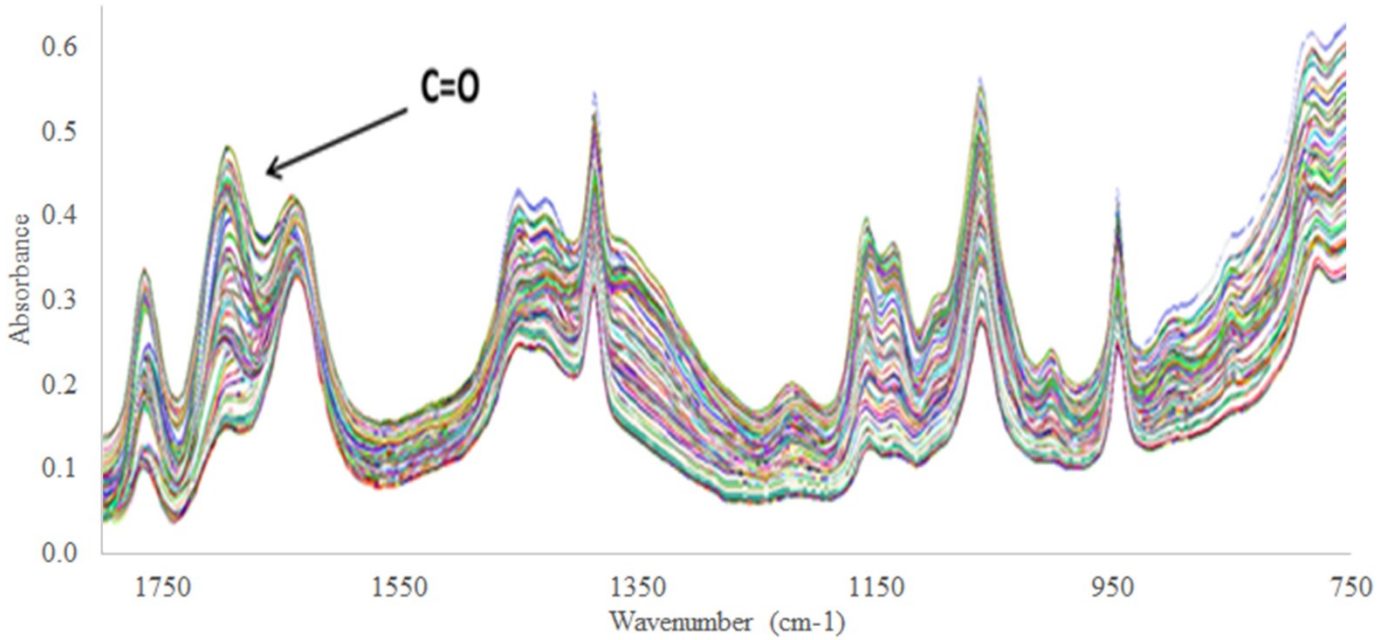

Figure 1.34. Overlay of a series of mid ATR-FTIR spectra for a fixed concentration solute-solvent system highlighting the effect of variable temperature across a wide spectral range.

Févotte and co-workers reported a calibration procedure for ATR-FTIR measurements applied to solution crystallisation processes [145]. This built on previous studies [146-148] that recognised the need to compensate for temperature sensitivity in the measurement due to inter- and intramolecular interactions. Although the univariate approach only used a correlation between an individual solute peak and solution concentration, the calibration had a maximal relative error of 2.3 % which can be of sufficient accuracy for practical application where more precise control is not required. Nagy and co-workers also reported a calibration procedure for ATR-UV monitoring and control [149]. The method used the first derivative of the absorbance spectra at two wavelengths and applied a simple nonlinear calibration function. Mahmud and co-workers reported a multivariate calibration procedure for the cooling crystallisation of L-glutamic acid with ATR-FTIR using partial least squares (PLS) to fit the calibration model [150]. A 5-factor model was developed and applied, with a typical percentage error of 4.79 %, highlighting PLS as an efficient approach in correcting for temperature dependent measurements.

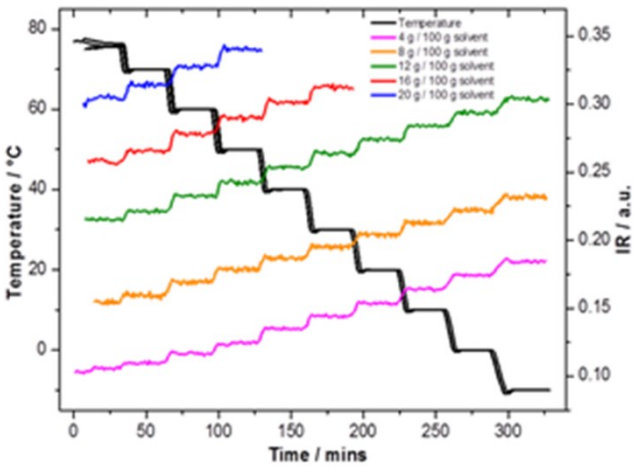

Figure 1.35. A full calibration data set for a given solute-solvent system. Five variable temperature experiments in the selected spectral range can be observed.

There are multiple physical transformations and hence rate parameters that dictate the actual performance of a crystallisation. Although rather sophisticated mathematical models have been published for some specific continuous pharmaceutical crystallisers, the vast majority of models for primary and secondary nucleation processes, size-dependent growth, phase transformations, attrition, agglomeration, and morphology rely on semi-empirical kinetic models. Obtaining reliable experimental kinetic data on these processes is a key step to inform robust process design and PAT can play a role in addition to traditional off line techniques. Indeed, the ability to collate relevant data in real time that describe the changes in temperature, solution concentration and particle number and size would be a major advance in accelerating process development.

Population balance models for example require accurate parameter estimates as well as particle size distributions that can be difficult to accurately measure in-situ using existing PAT sensors. Focused Beam Reflectance Measurement (FBRM) allows chord length measurement but has a non-unique relationship to the 3-dimensional particle size information that is actually required for these models. Nonetheless the FBRM probe is a powerful tool for the in-situ identification of nucleation (i.e. particle formation via increased particle counts) in crystallisation processes [133, 151]. The chord length distribution obtained from FBRM also provides information relating to the size and shape of particles that can be used to monitor and control growth [133], attrition [152] and agglomeration [153] processes. FBRM can also be used to provide information on the surface properties of crystals influencing their processability [154]. Inverse techniques to calculate the actual particle size distribution from the chord length distribution obtained from FBRM have also been developed and provide a basis for direct control of particle size distribution without the need for off line measurement of particle size and shape [155, 156]. Sensors have also been developed for in-situ monitoring of crystal shape but tend to be challenging to use or are only applicable for certain types of crystals [157]. Low cost web cameras have been demonstrated for non-invasive, in-situ monitoring of early signs of encrustation [158]. This approach used image analysis to develop a fouling metric indicator

that would allow early identification of the need for corrective actions during continuous crystallisation due to a build-up of crystals on the vessel walls or heat transfer surfaces.

1.5.2 Crystallisation Control Strategies

For the majority of crystallisation systems a basic feedback control strategy (e.g. PID, cascade) are designed to follow empirical operating policies (e.g. linear temperature profile, anti-solvent addition or evaporation rate) [159]. The advancement of in situ sensors and calibration methods has enabled precise real-time measurement of solute concentration (e.g. via ATR-FTIR, ATR-UV/Vis) and the characteristics of the crystal population's mass, size and morphology. This has enabled more advanced control strategies to be developed and applied [160], [49, 161, 162]. Generally these can be differentiated into two main categories: model-based and model-free control. However, increasingly hybrid control strategies have also been developed that combine model-based and model-free techniques.

1.5.2.1 Model-based control

The earliest examples of model-based control strategies demonstrated the benefits of using a programmed cooling profile which was calculated off line [163, 164]. Since then, major advances have allowed for the control of various aspects of product quality [165]. For a model-based optimization the solution must be constrained by the equipment limitations (e.g. maximum and minimum temperature values, maximum and minimal cooling rates, maximum volume, limits on anti-solvent addition rate, etc.) The crystallisation must also satisfy a productivity constraint that ensures the desired yield. Quality constraints can also be included such as those found in [166-168]. The effects of non-ideal mixing via computational fluid dynamics can also be incorporated [169].

Typically a model-based strategy will consist of:

1. The process model. This describes the product quality and process performance of the crystallisation. This is used either in real-time or off line to achieve the desired performance or quality. This will typically consist of the population balance equation, material and energy balances and the kinetic models for the crystallisation rate processes. The model should give a robust and accurate description of the crystallisation process in the selected crystalliser. Therefore, there is always the need to carry out parameter estimation and validation steps before it can be applied in the controller design.
2. A dynamic observer. Provides an estimate of the state of a real system from appropriate measurements. This is a crucial component of the model-based control strategy to achieve robust offset-free control. Different types of observers have been used in crystallisation control and a comparison between the different types of observers for crystallisation control has been performed [170].

3. A dynamic optimiser which is used to determine the optimal trajectory to reach the desired state of the process at the lowest possible cost. The efficiency and robustness of the optimiser therefore plays an important role in the design of the control system.

Model-based control strategies can provide the theoretically optimal operating conditions and generally require fewer experiments to develop, when properly designed, when compared to statistical experimental design. Model-based approaches also have the benefit of increased process understanding although this can be at the cost of development time and material to develop and validate the models. Of course, uncertainty will exist within the kinetic models given the ill-defined physics of some of the processes involved, and this needs to be taken into account to avoid poor performance of the controller when applied.

1.5.2.2 Model-free control

Model-free control approaches are based on the direct use of sensors or PAT-based measurements in feedback control of crystallisation processes. Whilst these approaches are based on defined models relating the response of the process to changes in process conditions, they are entirely empirical and do not assign any physical or mechanistic significance to the parameters. For example, for supersaturation control the objective is to control the crystallisation process by maintaining supersaturation at specific values at each stage of the process to enable a desired operating trajectory through the phase diagram [171, 172]. The state of the crystallisation process at any location in the process can be determined using actual concentration and temperature measurements and the concentration trajectory adjusted by varying the temperature. This approach provides the advantage that the operating curve can be defined based on prior understanding of the crystallisation process, to avoid triggering unwanted mechanisms, such as nucleation or polymorphic transformations by allowing the process to move out with the MSZW [173]. However, a controlled moved to out with the MSZW to initiate crystallisation followed by supersaturation control has been shown to be a valid strategy for particle size control [42, 172]. In the majority of reported applications, constant supersaturation is used for setpoint although the approach conceptually allows to specify more complex trajectories in the phase diagram. For example in the case of systems with complicated phase behaviour, e.g. with multiple forms (polymorphs, hydrates, solvates etc.) superaturation can be manipulated directly as required to maintain the desired form. The schematic representation of supersaturation control approach is shown in Figure 1.36.

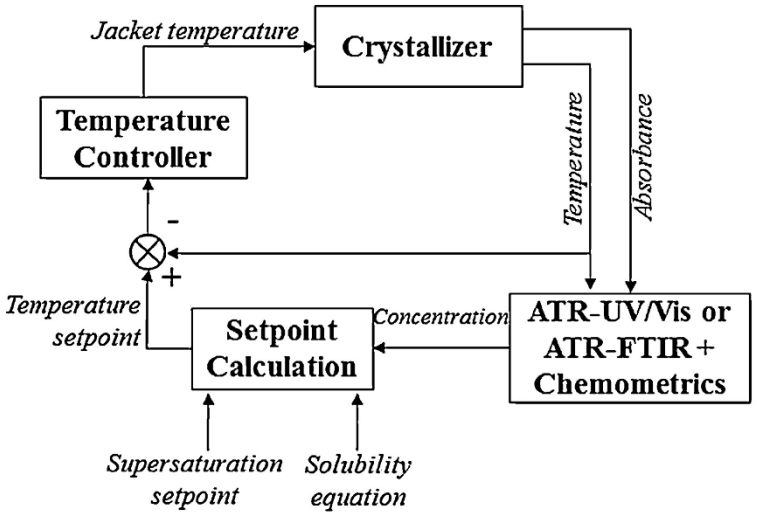

Figure 1.36. Schematic representation of the model-free control approaches for supersaturation control. Set points can be adjusted to maintain supersaturation at the required value in response to transients or fluctuations in the process. Reprinted from [173]. Copyright 2013, with permission from Elsevier.

Model-free control strategies can often result in close to optimal crystallisation performance though, just as with model based control approaches, it is important to understand the strengths and limitations of the model, the sensors being used and potential uncertainties that would result in the model operating out with sensible ranges. In the case of supersaturation control, particle attributes are not controlled directly and it may be possible for two separate crystallisation runs controlled at the same supersaturation to produce products with different attributes due to unmeasured disturbances including accidental seeding, attrition, agglomeration, fouling or variations in input materials. However, with validated models, reliable measurements and calibrations relating signals to required properties, robust process design and controlled input materials both model based and model free approaches can provide.

1.5.2.3 Hybrid strategies

A hybrid control strategy is one which combines features of both model-based and model-free strategies into a single strategy or utilizes one to generate data for the other. Although supersaturation control can produce high quality crystals, the setpoint for supersaturation is either arbitrarily chosen or found by trial and error. To address this issue Nagy and Aamir [174] incorporated an analytical solution of the population balance equation and a nonlinear optimization (model-based aspect) into the supersaturation control (model-free aspect) to find the optimal setpoint trajectory, in this case amount of seed, to target a specific size distribution shape, Figure 1.37. One key aspect of model-based strategies is the determination of the key process kinetic parameters in order to accurately model a given crystallisation system. There parameters are usually determined through fitting to well-designed experiments. Cao and co-workers [175] demonstrated the possibility of using supersaturation control to first generate high supersaturation for determination of nucleation kinetics, followed by low constant supersaturation for estimating growth kinetics. In order to determine a robust temperature/cooling profile which would not be subject to batch to batch variability of

the shape of the crystal size distribution, Nagy [176] developed a hierarchical structure with a low level supersaturation control (model-free approach) driving the system through the phase diagram, the set point of which was optimized at a higher level by solution of the population balance equation to counteract the effect of changing operating conditions.

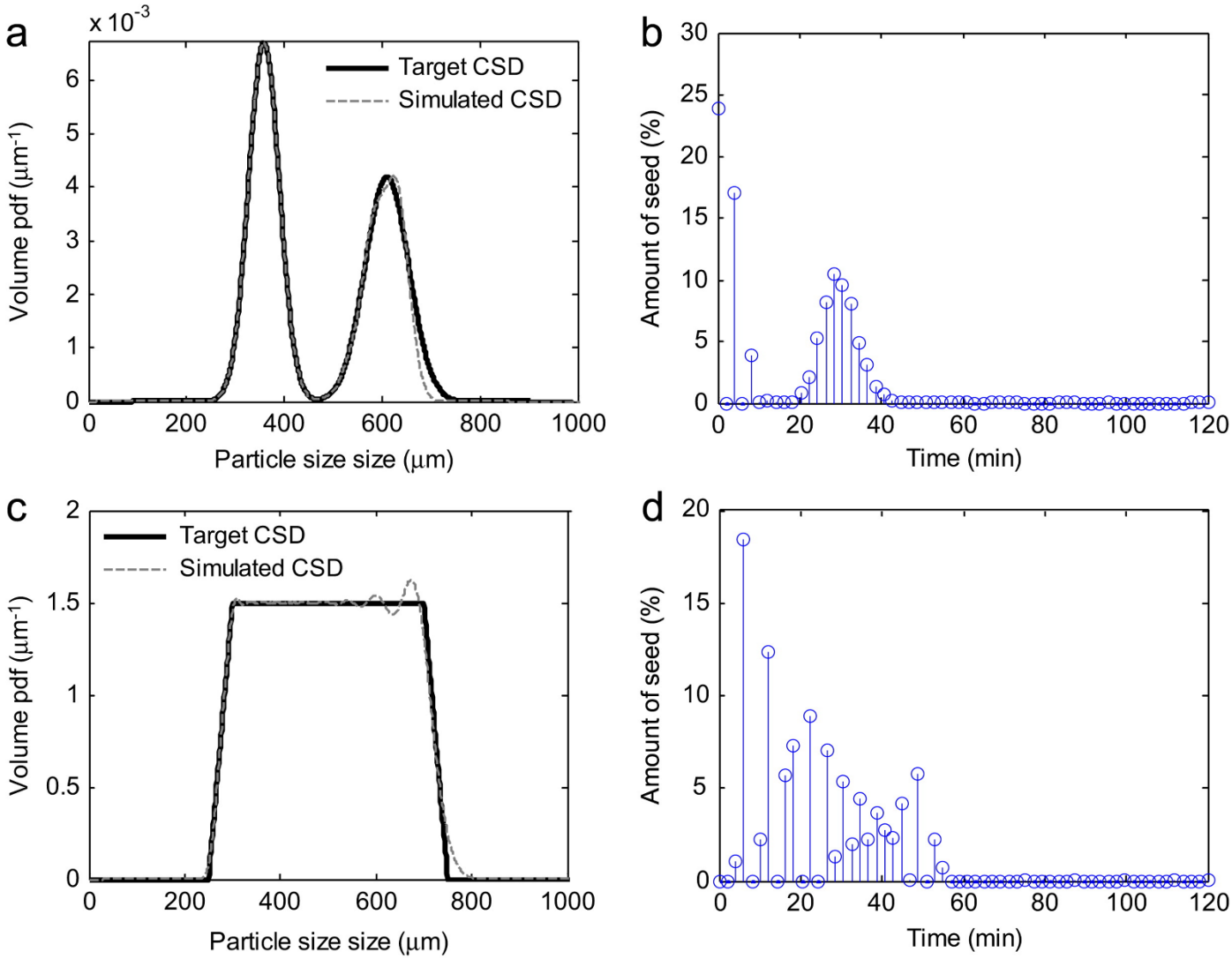

Figure 1.37. Results for the dynamic seed addition for bimodal and trapezoidal distributions (a) and (c) show the comparisons of target and simulated CSDs at the end of the batch, and (b) and (d) illustrate the dynamic seed addition profiles, with amount of seed in weight %. Reprinted from [174]. Copyright 2012, with permission from Elsevier.

1.6 Particle Characterisation

The development of robust continuous crystallisation processes requires a detailed understanding of how crystal quality is influenced by the process conditions and changes in key rate processes. Standard chemical and physical off line characterisation tools remain essential in this respect allowing samples of material taken at different positions from the continuous process to be analysed for chemical and physical consistency. This can inform on the dynamics of the process during early process development as well as during start-up, operation and shut-down to inform process design and control. There are a large number of analytical methods that may be used to determine the physical properties and structure of pharmaceutical

solids and it will often be necessary to combine data from several techniques in order to fully characterise a material [7, 177, 178].

Table 1.8. Summary of off line chemical and physical analytical techniques of value in the characterisation of pharmaceutical solids produced from crystallisation processes.

Analytical Method	Information provided
Optical Microscopy	Crystal morphology, colour, size and shape Lattice strain or twinning Identify presence of polymorphs from mixed morphologies
Laser diffraction	Determine Particle size distribution (PSD) for dry or wet dispersed particles Identify particle aggregation or agglomeration
DVS (dynamic vapour sorption)	Assess hygroscopicity from mass change as a function of %R.H. or organic vapour Identify structural transformations from non-solvated to solvated forms Mass loss on drying
Inverse gas phase chromatography	Measurement of particle surface energies Quantification of amorphous content
BET analysis	Specific surface area measurement of particulate materials Porosity of powder beds or formulated systems
Solubility / dissolution	Determine equilibrium saturation solubility and influence of pH, T and impurities Solution mediated phase transformations Dissolution rate (intrinsic dissolution rate)
SEM (scanning electron microscopy)	Morphology and surface structure of particles Influence of processing on particles Agglomeration and attrition of particles
AFM (atomic force microscopy)	Mechanical properties of crystal faces Surface topology and dynamics Surface roughness
Single crystal diffraction	Unit cell, space group atomic co-ordinates, displacement parameters 3-D molecular conformation and intermolecular packing Absolute configuration Morphology and indexing of crystal faces
X-ray powder diffraction (XRPD)	Phase identification for polycrystalline sample Quantitative analysis of composition of mixtures Unit cell, space group and atomic co-ordinates. Crystallinity in amorphous/crystalline mixed phase samples Size/strain analysis of particle microstructure Variable T and %R.H. studies

Mid FT-IR	Characteristic absorption spectrum for polymorphic forms Identify non-solvated and solvated forms Distinguish amorphous and crystalline forms Quantification of mixtures
Raman	Characteristic scattering spectrum for crystalline and amorphous forms Track lattice changes as a function of T and pressure Combine with microscopy for Raman mapping studies
Near IR	Characteristic absorption bands from O-H, C-H, and N-H stretches Detection of polymorphs and solvates Sensitive to water, useful for monitoring drying
Solid-state NMR	Determine number of unique formula units in unit cell Identify disorder Identify polymorphs and solvates
Terahertz spectroscopy	Molecular conformation and intermolecular packing Identify crystalline and amorphous solids Can combine with imaging
Differential scanning calorimetry (DSC)	Thermal transitions (desolvation; crystallisation; Tg; melt) Heat capacity, Cp, and heats of transition, ΔH Relative stabilities of polymorphs
Thermal gravimetric analysis (TGA)	Measure weight loss on heating associated with solvent loss Enable calculation of solvate stoichiometry
Melting point	Measure characteristic melting points for crystalline forms Assess purity
Hot-stage microscopy	Changes in particles as a function of T Structural transformations including desolvation Melting point
Solution NMR	Identification of molecular species from dissolved solid and mother liquor Sample purity Identification of impurities
GC/LC-MS	Chemical analysis of crystals and mother liquor Separate volatile (GC) or non-volatile (LC) components Identify impurities (MS)

1.7 Concluding Remarks

Continuous crystallisation offers the potential for flexible and effective control of particle attributes to achieve improved performance in formulation and final product application. This will require careful design and crystallisation control strategies to be developed and whilst significant progress has been made in these

areas, gaps in fundamental understanding of nucleation, growth and in crystal structure-property relationships and on the influence of process conditions on key transformations remain. Further developments in these areas will provide new opportunities to engineer particles with the required attributes to meet product performance needs by first intent and to design robust, scalable continuous processes to deliver them consistently.

There is also a need to develop and apply: (1) effective methods for gathering experimental physical data, quickly from limited material and (2) useful modelling tools to support process development and control. Equipment availability is also an important consideration and whilst there is a wide array of process technologies available, challenges also remain around standardisation, managing the presence of particles in flow, scalability, managing fouling and the need for effective, robust PAT for monitoring and controlling suspensions [179]. There is also a well recognised need to develop the right skills for the existing and future workforce to enable the implementation of continuous crystallisation processes to be fully realised including early implementation in development and through to manufacture.

1.8 References

1. Baxendale I.R., Braatz R.D., Hodnett B.K. *et al.* (2015) Achieving Continuous Manufacturing: Technologies and Approaches for Synthesis, Workup, and Isolation of Drug Substance May 20-21, 2014 Continuous Manufacturing Symposium. *Journal of Pharmaceutical Sciences,* **104**(3), 781-91
2. Badman C., Trout B.L. (2015) Achieving Continuous Manufacturing May 20-21, 2014 Continuous Manufacturing Symposium. *Journal of Pharmaceutical Sciences,* **104**(3), 779-80
3. Mascia S., Heider P.L., Zhang H.T. *et al.* (2013) End-to-End Continuous Manufacturing of Pharmaceuticals: Integrated Synthesis, Purification, and Final Dosage Formation. *Angew Chem-Int Edit,* **52**(47), 12359-63
4. Adamo A., Beingessner R.L., Behnam M. *et al.* (2016) On-demand continuous-flow production of pharmaceuticals in a compact, reconfigurable system. *Science,* **352**(6281), 61-7
5. Variankaval N., Cote A.S., Doherty M.F. (2008) From form to function: Crystallization of active pharmaceutical ingredients. *Aiche Journal,* **54**(7), 1682-8
6. Chen J., Sarma B., Evans J.M.B., Myerson A.S. (2011) Pharmaceutical Crystallization. *Crystal Growth & Design,* **11**(4), 887-95
7. Florence A.J. (2009) The Solid State, in *Modern Pharmaceutics*, 5th edn, vol. 1 (eds Florence A., Siepmann J.), New York, USA, pp. 253-310
8. Winn D., Doherty M.F. (2000) Modeling crystal shapes of organic materials grown from solution. *Aiche J,* **46**(7), 1348-67
9. Randolph A.D. (1969) Effect of Crystal Breakage on Crystal Size Distribution in a MIxed Suspension Crystallizer. *Industrial & Engineering Chemistry Fundamentals,* **8**(1), 58-63
10. Reddy C.M., Padmanabhan K.A., Desiraju G.R. (2006) Structure-property correlations in bending and brittle organic crystals. *Crystal Growth & Design,* **6**(12), 2720-31
11. Brunsteiner M., Jones A.G., Pratola F. *et al.* (2005) Toward a molecular understanding of crystal agglomeration. *Crystal Growth & Design,* **5**(1), 3-16
12. Tavare N.S. (1986) Mixing in Continuous Crystallizers. *Aiche Journal,* **32**(5), 705-32
13. Castagnoli C., Yahyah M., Cimarosti Z., Peterson J.J. (2010) Application of Quality by Design Principles for the Definition of a Robust Crystallization Process for Casopitant Mesylate. *Org Process Res Dev,* **14**(6), 1415-27
14. Yu L.X. (2008) Pharmaceutical quality by design: Product and process development, understanding, and control. *Pharm Res,* **25**(4), 781-91
15. Jiang M., Wong M.H., Zhu Z. *et al.* (2012) Towards achieving a flattop crystal size distribution by continuous seeding and controlled growth. *Chemical Engineering Science,* **77**, 2-9
16. Lawton S., Steele G., Shering P. *et al.* (2009) Continuous Crystallization of Pharmaceuticals Using a Continuous Oscillatory Baffled Crystallizer. *Organic Process Research & Development,* **13**(6), 1357-63

17. Schaber S.D., Gerogiorgis D.I., Ramachandran R. *et al.* (2011) Economic analysis of integrated continuous and batch pharmaceutical manufacturing: a case study. *Industrial & Engineering Chemistry Research,* **50**(17), 10083-92
18. McGlone T., Briggs N.E.B., Clark C.A. *et al.* (2015) Oscillatory Flow Reactors (OFRs) for Continuous Manufacturing and Crystallization. *Organic Process Research & Development,* **19**(9), 1186-202
19. Alvarez A.J., Singh A., Myerson A.S. (2011) Crystallization of Cyclosporine in a Multistage Continuous MSMPR Crystallizer. *Cryst Growth Des,* **11**(10), 4392-400
20. Su Q., Nagy Z.K., Rielly C.D. (2015) Pharmaceutical crystallisation processes from batch to continuous operation using MSMPR stages: Modelling, design, and control. *Chemical Engineering and Processing: Process Intensification,* **89**, 41-53
21. Lai T.-T.C., Cornevin J., Ferguson S. *et al.* (2015) Control of Polymorphism in Continuous Crystallization via Mixed Suspension Mixed Product Removal Systems Cascade Design. *Cryst Growth Des,* **15**(7), 3374-82
22. Zhang H., Quon J., Alvarez A.J. *et al.* (2012) Development of Continuous Anti-Solvent/Cooling Crystallization Process using Cascaded Mixed Suspension, Mixed Product Removal Crystallizers. *Org Process Res Dev,* **16**(5), 915-24
23. Ferguson S., Morris G., Hao H. *et al.* (2013) Characterization of the anti-solvent batch, plug flow and MSMPR crystallization of benzoic acid. *Chemical Engineering Science,* **104**, 44-54
24. Ricardo C., Xiongwei N. (2009) Evaluation and Establishment of a Cleaning Protocol for the Production of Vanisal Sodium and Aspirin Using a Continuous Oscillatory Baffled Reactor. *Organic Process Research & Development,* **13**(6), 1080-7
25. Lobry E., Lasuye T., Gourdon C., Xuereb C. (2015) Liquid–liquid dispersion in a continuous oscillatory baffled reactor–Application to suspension polymerization. *Chemical Engineering Journal,* **259**, 505-18
26. Konig C., Bechtold-Peters K., Baum V. *et al.* (2012) Development of a pilot-scale manufacturing process for protein-coated microcrystals (PCMC): Mixing and precipitation - Part I. *Eur J Pharm Biopharm,* **80**(3), 490-8
27. Alvarez A.J., Myerson A.S. (2010) Continuous Plug Flow Crystallization of Pharmaceutical Compounds. *Cryst Growth Des,* **10**(5), 2219-28
28. Eder R.J.P., Schrank S., Besenhard M.O. *et al.* (2012) Continuous Sonocrystallization of Acetylsalicylic Acid (ASA): Control of Crystal Size. *Crystal Growth & Design,* **12**(10), 4733-8
29. Narducci O., Jones A.G., Kougoulos E. (2011) Continuous crystallization of adipic acid with ultrasound. *Chemical Engineering Science,* **66**(6), 1069-76
30. Eden R.J.P., Radl S., Schmitt E. *et al.* (2010) Continuously Seeded, Continuously Operated Tubular Crystallizer for the Production of Active Pharmaceutical Ingredients. *Crystal Growth & Design,* **10**(5), 2247-57

31. Wong S.Y., Tatusko A.P., Trout B.L., Myerson A.S. (2012) Development of Continuous Crystallization Processes Using a Single-Stage Mixed-Suspension, Mixed-Product Removal Crystallizer with Recycle. *Cryst Growth Des,* **12**(11), 5701-7
32. Wierzbowska B., Hutnik N., Piotrowski K., Matynia A. (2011) Continuous Mass Crystallization of Vitamin C in L(+)-Ascorbic Acid-Ethanol-Water System: Size-Independent Growth Kinetic Model Approach. *Crystal Growth & Design,* **11**(5), 1557-65
33. Quon J.L., Zhang H., Alvarez A. *et al.* (2012) Continuous Crystallization of Aliskiren Hemifumarate. *Crystal Growth & Design,* **12**(6), 3036-44
34. Wong S.Y., Cui Y.Q., Myerson A.S. (2013) Contact Secondary Nucleation as a Means of Creating Seeds for Continuous Tubular Crystallizers. *Crystal Growth & Design,* **13**(6), 2514-21
35. Mersmann A. (2001) *Crystallization Technology Handbook,* 2nd edn, Marcel Dekker, New York
36. Mullin J.W. (2001) *Crystallization,* 4th edn, Butterworth-Heinemann, Oxford
37. Davey R.J., Garside J. (2000) *From molecules to crystallizers,* Oxford University Press, Oxford
38. Myerson A.S. (2002) *Handbook of Industrial Crystallization,* 2nd edn, Butterworth-Heinemann, Woburn
39. Gilbert S.W. (1991) Melt Crystallization - Process Analysis and Optimization. *Aiche Journal,* **37**(8), 1205-18
40. Rittner S., Steiner R. (1985) Melt Crystallization of Organic-Substances and Its Large-Scale Application. *Chem-Ing-Tech,* **57**(2), 91-102
41. Beckmann W. (2013) *Crystallization: Basic Concepts and Industrial Applications,* Wiley
42. Saleemi A., Rielly C., Nagy Z.K. (2012) Automated direct nucleation control for in situ dynamic fines removal in batch cooling crystallization. *Crystengcomm,* **14**(6), 2196-203
43. Brito A.B.N., Giulietti M. (2007) Study of lactose crystallization in water-acetone solutions. *Crystal Research and Technology,* **42**(6), 583-8
44. Muller F.L., Fielding M., Black S. (2009) A Practical Approach for Using Solubility to Design Cooling Crystallisations. *Organic Process Research & Development,* **13**(6), 1315-21
45. Lindenberg C., Krattli M., Cornel J. *et al.* (2009) Design and Optimization of a Combined Cooling/Antisolvent Crystallization Process. *Crystal Growth & Design,* **9**(2), 1124-36
46. Nagy Z.K., Fujiwara M., Braatz R.D. (2008) Modelling and control of combined cooling and antisolvent crystallization processes. *Journal of Process Control,* **18**(9), 856-64
47. Jones H.P., Davey R.J., Cox B.G. (2005) Crystallization of a salt of a weak organic acid and base: Solubility relations, supersaturation control and polymorphic behavior. *J Phys Chem B,* **109**(11), 5273-8
48. Kim S.T., Kwon J.H., Lee J.J., Kim C.W. (2003) Microcrystallization of indomethacin using a pH-shift method. *International Journal of Pharmaceutics,* **263**(1-2), 141-50

49. Mesbah A., Huesman A.E.M., Kramer H.J.M. *et al.* (2011) Real-time control of a semi-industrial fed-batch evaporative crystallizer using different direct optimization strategies. *AIChE Journal,* **57**(6), 1557-69
50. Fages J., Lochard H., Letourneau J.J. *et al.* (2004) Particle generation for pharmaceutical applications using supercritical fluid technology. *Powder Technology,* **141**(3), 219-26
51. Söhnel O., Garside J. (1992) *Precipitation: Basic Principles and Industrial Applications,* Butterworth-Heinemann
52. Garside J., Davey R.J. (1980) Secondary Contact Nucleation - Kinetics, Growth and Scale-Up. *Chemical Engineering Communications,* **4**(4-5), 393-424
53. Mersmann A.S., R.; Kind, M.; Pohlisch, J. (1988) Attrition and secondary nucleation in crystallizers. *Chem Eng Technol,* **11**(1), 80-8
54. Nývlt J. (1968) Kinetics of nucleation in solutions. *Journal of Crystal Growth,* **3–4**, 377-83
55. Sangwal K. (2011) Some features of metastable zone width of various systems determined by polythermal method. *Crystengcomm,* **13**(2), 489-501
56. Kashchiev D., Borissova A., Hammond R.B., Roberts K.J. (2010) Effect of cooling rate on the critical undercooling for crystallization. *Journal of Crystal Growth,* **312**(5), 698-704
57. Kobari M., Kubota N., Hirasawa I. (2013) Deducing primary nucleation parameters from metastable zone width and induction time data determined with simulation. *Crystengcomm,* **15**(6), 1199-209
58. Larson M.A. (1981) Secondary Nucleation - an Analysis. *Chemical Engineering Communications,* **12**(1-3), 161-9
59. Chianese A., Diberardino F., Jones A.G. (1993) On the Effect of Secondary Nucleation on the Crystal Size Distribution from a Seeded Batch Crystallizer. *Chemical Engineering Science,* **48**(3), 551-60
60. Brandel C., ter Horst J.H. (2015) Measuring induction times and crystal nucleation rates. *Faraday Discuss,* **179**, 199-214
61. Jiang S.F., ter Horst J.H. (2011) Crystal Nucleation Rates from Probability Distributions of Induction Times. *Crystal Growth & Design,* **11**(1), 256-61
62. Kulkarni S.A., Kadam S.S., Meekes H. *et al.* (2013) Crystal Nucleation Kinetics from Induction Times and Metastable Zone Widths. *Crystal Growth & Design,* **13**(6), 2435-40
63. Davey R.J., Back K.R., Sullivan R.A. (2015) Crystal nucleation from solutions - transition states, rate determining steps and complexity. *Faraday Discuss,* **179**, 9-26
64. Dunning W.J.S., A. J. *Nucleation in sucrose solutions.* Proceedings of the Proc Agric Industries 10th International Conference, 1954, Madrid,
65. Davey R.J.S., S. L.; ter Horst, J. H. (2013) Nucleation of organic crystals - a molecular perspective. *Angew Chem In Ed,* **52**(8), 2166-79
66. Erdemir D., Lee A.Y., Myerson A.S. (2009) Nucleation of Crystals from Solution: Classical and Two-Step Models. *Accounts Chem Res,* **42**(5), 621-9

67. Briggs N.E.B. Polymorph control of pharmaceuticals within a continuous oscillatory baffled crystalliser: Thesis [Ph. D] --University of Strathclyde, 2015; 2015.
68. Beckman J.R., Randolph A.D. (1977) Crystal size distribution dynamics in a classified crystallizer: Part II. Simulated control of crystal size distribution. *AIChE Journal,* **23**(4), 510-20
69. Garside J., Jancic S.J. (1978) Prediction and Measurement of Crystal Size Distribution for Size-Dependent Growth. *Chemical Engineering Science,* **33**(12), 1623-30
70. Garside J. (1985) Industrial Crystallization from Solution. *Chemical Engineering Science,* **40**(1), 3-26
71. Alander E.M., Rasmuson A.C. (2005) Mechanisms of crystal agglomeration of paracetamol in acetone-water mixtures. *Industrial & Engineering Chemistry Research,* **44**(15), 5788-94
72. Kawashima Y., Imai A., Takeuchi H. *et al.* (2003) Improved flowability and compactibility of spherically agglomerated crystals of ascorbic acid for direct tableting designed by spherical crystallization process. *Powder Technology,* **130**(1-3), 283-9
73. Randolph A.D., Larson M.A. (1988) *Theory of particulate processes: analysis and techniques of continuous crystallization,* 2nd edn, Academic Press, London
74. Myerson A.S., Krumme M., Nasr M. *et al.* (2015) Control Systems Engineering in Continuous Pharmaceutical Manufacturing May 20-21, 2014 Continuous Manufacturing Symposium. *Journal of Pharmaceutical Sciences,* **104**(3), 832-9
75. Yang Y., Nagy Z.K. (2015) Combined Cooling and Antisolvent Crystallization in Continuous Mixed Suspension, Mixed Product Removal Cascade Crystallizers: Steady-State and Startup Optimization. *Industrial & Engineering Chemistry Research,* **54**(21), 5673-82
76. Bermingham S.K., Neumann A.M., Kramer H.J.M. *et al.* (2000) A design procedure and predictive models for solution crystallisation processes. *Aiche Sym S,* **96**(323), 250-64
77. Jolliffe H.G., Gerogiorgis D.I. (2015) Process modelling and simulation for continuous pharmaceutical manufacturing of ibuprofen. *Chem Eng Res Des,* **97**, 175-91
78. Vetter T., Burcham C.L., Doherty M.F. (2015) Designing Robust Crystallization Processes in the Presence of Parameter Uncertainty Using Attainable Regions. *Industrial & Engineering Chemistry Research,* **54**(42), 10350-63
79. Shaikh L.J., Bari A.H., Ranade V.V., Pandit A.B. (2015) Generic Framework for Crystallization Processes Using the Population Balance Model and Its Applicability. *Industrial & Engineering Chemistry Research,* **54**(42), 10539-48
80. Teoh S.K., Rathi C., Sharratt P. (2016) Practical Assessment Methodology for Converting Fine Chemicals Processes from Batch to Continuous. *Organic Process Research & Development,* **20**(2), 414-31
81. Cheng Y.S., Lam K.W., Ng K.M., Wibowo C. (2010) Workflow for Managing Impurities in an Integrated Crystallization Process. *Aiche Journal,* **56**(3), 633-49
82. ICH Guideline Q3C (R5) on Impurities: Guideline for Residual Solvents, (2011).

83. Siddique H., Brown C.J., Houson I., Florence A.J. (2015) Establishment of a Continuous Sonocrystallization Process for Lactose in an Oscillatory Baffled Crystallizer. *Organic Process Research & Development,* **19**(12), 1871-81
84. Kirwan D.J., Orella C.J. (2002) Crystallization in the pharmaceutical and bioprocessing industries, in *Handbook of Industrial Crystallization*, 2nd edn, (eds Myerson A.S.), Butterworth-Heinemann, Woburn, pp. 249-66
85. Vetter T., Burcham C.L., Doherty M.F. (2014) Regions of attainable particle sizes in continuous and batch crystallization processes. *Chemical Engineering Science,* **106**, 167-80
86. Levenspiel O. (1999) *Chemical reaction engineering,* Wiley
87. Powell K.A., Saleemi A.N., Rielly C.D., Nagy Z.K. (2015) Periodic steady-state flow crystallization of a pharmaceutical drug using MSMPR operation. *Chemical Engineering and Processing: Process Intensification,* **97**, 195-212
88. Chemaly Z., Muhr H., Fick M. (1999) Crystallization kinetics of calcium lactate in a Mixed-Suspension-Mixed-Product Removal crystallizer. *Industrial & Engineering Chemistry Research,* **38**(7), 2803-8
89. Ferguson S., Ortner F., Quon J. *et al.* (2014) Use of Continuous MSMPR Crystallization with Integrated Nanofiltration Membrane Recycle for Enhanced Yield and Purity in API Crystallization. *Crystal Growth & Design,* **14**(2), 617-27
90. Gerard A., Muhr H., Plasari E. *et al.* (2014) Effect of calcium based additives on the sodium bicarbonate crystallization in a MSMPR reactor. *Powder Technology,* **255**, 134-40
91. Hou G., Power G., Barrett M. *et al.* (2014) Development and Characterization of a Single Stage Mixed-Suspension, Mixed-Product-Removal Crystallization Process with a Novel Transfer Unit. *Crystal Growth & Design,* **14**(4), 1782-93
92. Yang Y., Song L., Gao T., Nagy Z.K. (2015) Integrated Upstream and Downstream Application of Wet Milling with Continuous Mixed Suspension Mixed Product Removal Crystallization. *Crystal Growth & Design,* **15**(12), 5879-85
93. Kozik A., Hutnik N., Piotrowski K., Matynia A. (2014) Continuous reaction crystallization of struvite from diluted aqueous solution of phosphate(V) ions in the presence of magnesium ions excess. *Chemical Engineering Research and Design,* **92**(3), 481-90
94. Hutnik N., Piotrowski K., Wierzbowska B., Matynia A. (2011) Continuous reaction crystallization of struvite from phosphate(V) solutions containing calcium ions. *Crystal Research and Technology,* **46**(5), 443-9
95. Lai T.-T.C., Ferguson S., Palmer L. *et al.* (2014) Continuous Crystallization and Polymorph Dynamics in the l-Glutamic Acid System. *Organic Process Research & Development,* **18**(11), 1382-90
96. Tai C.Y., Shei W.-L. (1993) Crystallization kinetics and product purity of α-glutamic acid crystal. *Chemical Engineering Communications,* **120**(1), 139-52

97. Wierzbowska B., Hutnik N., Piotrowski K., Matynia A. (2011) Continuous Mass Crystallization of Vitamin C in l(+)-Ascorbic Acid−Ethanol−Water System: Size-Independent Growth Kinetic Model Approach. *Crystal Growth & Design,* **11**(5), 1557-65

98. Wierzbowska B., Koralewska J., Piotrowski K. *et al.* (2008) Kinetic aspects of a continuous mode of mass crystallization of vitamin C in the l(+)-ascorbic acid-methanol-water system. *Chemical and Process Engineering-Inzynieria Chemiczna I Procesowa,* **29**(2), 345-60

99. Wierzbowska B., Piotrowski K., Hutnik N., Matynia A. (2008) Continuous crystallization of vitamin C in L(+)-ascorbic acid-methanol-water system. An SDG kinetic model approach. *Chemical and Process Engineering-Inzynieria Chemiczna I Procesowa,* **29**(4), 1083-94

100. Wierzbowska B., Piotrowski K., Koralewska J. *et al.* (2009) Kinetics of nucleation and growth of L-sorbose crystals in a continuous MSMPR crystallizer with draft tube: Size-independent growth model approach. *Korean J Chem Eng,* **26**(1), 175-81

101. Power G., Hou G., Kamaraju V.K. *et al.* (2015) Design and optimization of a multistage continuous cooling mixed suspension, mixed product removal crystallizer. *Chemical Engineering Science,* **133**, 125-39

102. Peña R., Nagy Z.K. (2015) Process Intensification through Continuous Spherical Crystallization Using a Two-Stage Mixed Suspension Mixed Product Removal (MSMPR) System. *Crystal Growth & Design,* **15**(9), 4225-36

103. Galan K., Eicke M.J., Elsner M.P. *et al.* (2015) Continuous Preferential Crystallization of Chiral Molecules in Single and Coupled Mixed-Suspension Mixed-Product-Removal Crystallizers. *Crystal Growth & Design,* **15**(4), 1808-18

104. Zhao L., Raval V., Briggs N.E.B. *et al.* (2014) From discovery to scale-up: α-lipoic acid : nicotinamide co-crystals in a continuous oscillatory baffled crystalliser. *CrystEngComm,* **16**(26), 5769-80

105. Brown C.J., Adelakun J.A., Ni X.-w. (2015) Characterization and modelling of antisolvent crystallization of salicylic acid in a continuous oscillatory baffled crystallizer. *Chemical Engineering and Processing: Process Intensification,* **97**, 180-6

106. Ferguson S., Morris G., Hao H. *et al.* (2012) In-situ monitoring and characterization of plug flow crystallizers. *Chemical Engineering Science,* **77**, 105-11

107. Briggs N.E.B., Schacht U., Raval V. *et al.* (2015) Seeded Crystallization of β-l-Glutamic Acid in a Continuous Oscillatory Baffled Crystallizer. *Organic Process Research & Development,* **19**(12), 1903-11

108. Eder R.J.P., Schmitt E.K., Grill J. *et al.* (2011) Seed loading effects on the mean crystal size of acetylsalicylic acid in a continuous-flow crystallization device. *Crystal Research and Technology,* **46**(3), 227-37

109. Tari T., Fekete Z., Szabó-Révész P., Aigner Z. (2015) Reduction of glycine particle size by impinging jet crystallization. *International Journal of Pharmaceutics,* **478**(1), 96-102

110. Jiang M., Li Y.-E.D., Tung H.-H., Braatz R.D. (2015) Effect of jet velocity on crystal size distribution from antisolvent and cooling crystallizations in a dual impinging jet mixer. *Chemical Engineering and Processing: Process Intensification,* **97**, 242-7
111. Ildefonso M., Revalor E., Punniam P. *et al.* (2012) Nucleation and polymorphism explored via an easy-to-use microfluidic tool. *Journal of Crystal Growth,* **342**(1), 9-12
112. Goyal S., Economou A.E., Papadopoulos T. *et al.* (2016) Solvent compatible microfluidic platforms for pharmaceutical solid form screening. *RSC Advances,* **6**(16), 13286-96
113. Leng J., Salmon J.-B. (2009) Microfluidic crystallization. *Lab on a Chip,* **9**(1), 24-34
114. Ildefonso M., Candoni N., Veesler S. (2012) A Cheap, Easy Microfluidic Crystallization Device Ensuring Universal Solvent Compatibility. *Organic Process Research & Development,* **16**(4), 556-60
115. Zhang S., Ferté N., Candoni N., Veesler S. (2015) Versatile Microfluidic Approach to Crystallization. *Organic Process Research & Development,* **19**(12), 1837-41
116. Simon L.L., Pataki H., Marosi G. *et al.* (2015) Assessment of Recent Process Analytical Technology (PAT) Trends: A Multiauthor Review. *Organic Process Research & Development,* **19**(1), 3-62
117. Barrett P., Smith B., Worlitschek J. *et al.* (2005) A review of the use of process analytical technology for the understanding and optimization of production batch crystallization processes. *Organic Process Research & Development,* **9**(3), 348-55
118. Nagy Z.K., Fevotte G., Kramer H., Simon L.L. (2013) Recent advances in the monitoring, modelling and control of crystallization systems. *Chem Eng Res Des,* **91**(10), 1903-22
119. Yu L.X., Lionberger R.A., Raw A.S. *et al.* (2004) Applicatlons of process analytical technology to crystallization processes. *Advanced Drug Delivery Reviews,* **56**(3), 349-69
120. Billot P., Couty M., Hosek P. (2010) Application of ATR-UV Spectroscopy for Monitoring the Crystallisation of UV Absorbing and Nonabsorbing Molecules. *Organic Process Research & Development,* **14**(3), 511-23
121. Helmdach L., Feth M.P., Ulrich J. (2013) Integration of Process Analytical Technology Tools in Pilot-Plant Setups for the Real-Time Monitoring of Crystallizations and Phase Transitions. *Organic Process Research & Development,* **17**(3), 585-98
122. Saleemi A.N., Rielly C.D., Nagy Z.K. (2012) Monitoring of the combined cooling and antisolvent crystallisation of mixtures of aminobenzoic acid isomers using ATR-UV/vis spectroscopy and FBRM. *Chemical Engineering Science,* **77**, 122-9
123. Henry M., Puel F.E., Perrichon P.D. *et al.* (2008) SGGP 2007 - Understanding and modelling of crystallization mechanisms by in-situ analytical technologies monitoring. *Int J Chem React Eng,* **6**,
124. Pollanen K., Hakkinen A., Reinikainen S.P. *et al.* (2005) IR spectroscopy together with multivariate data analysis as a process analytical tool for in-line monitoring of crystallization process and solid-state analysis of crystalline product. *J Pharmaceut Biomed,* **38**(2), 275-84

125. Pataki H., Markovits I., Vajna B. *et al.* (2012) In-Line Monitoring of Carvedilol Crystallization Using Raman Spectroscopy. *Crystal Growth & Design,* **12**(11), 5621-8
126. Qu H.Y., Louhi-Kultanen M., Kallas J. (2007) Additive effects on the solvent-mediated anhydrate/hydrate phase transformation in a mixed solvent. *Crystal Growth & Design,* **7**(4), 724-9
127. Scholl J., Bonalumi D., Vicum L. *et al.* (2006) In situ monitoring and modeling of the solvent-mediated polymorphic transformation of L-glutamic acid. *Crystal Growth & Design,* **6**(4), 881-91
128. Barrett M., McNamara M., Hao H.X. *et al.* (2010) Supersaturation tracking for the development, optimization and control of crystallization processes. *Chem Eng Res Des,* **88**(8A), 1108-19
129. Duffy D., Barrett M., Glennon B. (2013) Novel, Calibration-Free Strategies for Supersaturation Control in Antisolvent Crystallization Processes. *Crystal Growth & Design,* **13**(8), 3321-32
130. Gron H., Borissova A., Roberts K.J. (2003) In-process ATR-FTIR spectroscopy for closed-loop supersaturation control of a batch crystallizer producing monosodium glutamate crystals of defined size. *Industrial & Engineering Chemistry Research,* **42**(1), 198-206
131. Liotta V., Sabesan V. (2004) Monitoring and feedback control of supersaturation using ATR-FTIR to produce an active pharmaceutical ingredient of a desired crystal size. *Organic Process Research & Development,* **8**(3), 488-94
132. Pataki H., Csontos I., Nagy Z.K. *et al.* (2013) Implementation of Raman Signal Feedback to Perform Controlled Crystallization of Carvedilol. *Org Process Res Dev,* **17**(3), 493-9
133. Abu Bakar M.R., Nagy Z.K., Saleemi A.N., Rielly C.D. (2009) The Impact of Direct Nucleation Control on Crystal Size Distribution in Pharmaceutical Crystallization Processes. *Crystal Growth & Design,* **9**(3), 1378-84
134. Saleemi A.N., Steele G., Pedge N.I. *et al.* (2012) Enhancing crystalline properties of a cardiovascular active pharmaceutical ingredient using a process analytical technology based crystallization feedback control strategy. *International Journal of Pharmaceutics,* **430**(1-2), 56-64
135. Chen Z.P., Morris J., Martin E. (2005) Correction of temperature-induced spectral variations by loading space standardization. *Anal Chem,* **77**(5), 1376-84
136. Du W., Chen Z.P., Zhong L.J. *et al.* (2011) Maintaining the predictive abilities of multivariate calibration models by spectral space transformation. *Anal Chim Acta,* **690**(1), 64-70
137. Rajalahti T., Kvalheim O.M. (2011) Multivariate data analysis in pharmaceutics: A tutorial review. *International Journal of Pharmaceutics,* **417**(1-2), 280-90
138. Haaland D.M. (2000) Synthetic multivariate models to accommodate unmodeled interfering spectral components during quantitative spectral analyses. *Appl Spectrosc,* **54**(2), 246-54
139. Swierenga H., Wulfert F., de Noord O.E. *et al.* (2000) Development of robust calibration models in near infra-red spectrometric applications. *Anal Chim Acta,* **411**(1-2), 121-35
140. Wang Y.D., Kowalski B.R. (1993) Temperature-Compensating Calibration Transfer for near-Infrared Filter Instruments. *Anal Chem,* **65**(9), 1301-3

141. Wulfert F., Kok W.T., Smilde A.K. (1998) Influence of temperature on vibrational spectra and consequences for the predictive ability of multivariate models. *Anal Chem,* **70**(9), 1761-7
142. Barring H.K., Boelens H.F.M., de Noord O.E., Smilde A.K. (2001) Optimizing meta-parameters in continuous piecewise direct standardization. *Appl Spectrosc,* **55**(4), 458-66
143. Wulfert F., Kok W.T., de Noord O.E., Smilde A.K. (2000) Correction of temperature-induced spectral variation by continuous piecewise direct standardization. *Anal Chem,* **72**(7), 1639-44
144. Chen Z.P., Morris J. (2008) Improving the linearity of spectroscopic data subjected to fluctuations in external variables by the extended loading space standardization. *Analyst,* **133**(7), 914-22
145. Lewiner F., Klein J.P., Puel F., Fevotte G. (2001) On-line ATR FTIR measurement of supersaturation during solution crystallization processes. Calibration and applications on three solute/solvent systems. *Chemical Engineering Science,* **56**(6), 2069-84
146. Dunuwila D.B., K. A. (1996) ATR FTIR spectroscopy for in situ analysis of crystallization. *Proceedings of the 13th symposium on industrial crystallization,* **Toulouse**,
147. Dunuwila D.D., Berglund K.A. (1997) ATR FTIR spectroscopy for in situ measurement of supersaturation. *Journal of Crystal Growth,* **179**(1-2), 185-93
148. Groen H.R., K. J. (1999) Application of ATR FTIR spectroscopy for on-line determination of solute concentration and solution supersaturation. *Proceedings of the 14th international symposium on industrial crystallization,* **Cambridge**,
149. Simone E., Saleemi A.N., Tonnon N., Nagy Z.K. (2014) Active Polymorphic Feedback Control of Crystallization Processes Using a Combined Raman and ATR-UV/Vis Spectroscopy Approach. *Crystal Growth & Design,* **14**(4), 1839-50
150. Borissova A., Khan S., Mahmud T. *et al.* (2009) In Situ Measurement of Solution Concentration during the Batch Cooling Crystallization of L-Glutamic Acid using ATR-FTIR Spectroscopy Coupled with Chemometrics. *Crystal Growth & Design,* **9**(2), 692-706
151. Barrett P., Glennon B. (2002) Characterizing the metastable zone width and solubility curve using lasentec FBRM and PVM. *Chem Eng Res Des,* **80**(A7), 799-805
152. Kougoulos E., Jones A.G., Wood-Kaczmar M.W. (2005) Modelling particle disruption of an organic fine chemical compound using Lasentec focussed beam reflectance monitoring (FBRM) in agitated suspensions. *Powder Technology,* **155**(2), 153-8
153. Yu Z.Q., Tan R.B.H., Chow P.S. (2005) Effects of operating conditions on agglomeration and habit of paracetamol crystals in anti-solvent crystallization. *Journal of Crystal Growth,* **279**(3-4), 477-88
154. Abu Bakar M.R., Nagy Z.K., Rielly C.D. (2010) Investigation of the Effect of Temperature Cycling on Surface Features of Sulfathiazole Crystals during Seeded Batch Cooling Crystallization. *Crystal Growth & Design,* **10**(9), 3892-900
155. Worlitschek J., Mazzotti M. (2004) Model-based optimization of particle size distribution in batch-cooling crystallization of paracetamol. *Cryst Growth Des,* **4**(5), 891-903

156. Agimelen O.S., Hamilton P., Haley I. *et al.* (2015) Estimation of particle size distribution and aspect ratio of non-spherical particles from chord length distribution. *Chemical Engineering Science,* **123**, 629-40
157. Nagy Z.K., Braatz R.D. (2012) Advances and new directions in crystallization control. *Annu Rev Chem Biomol Eng,* **3**(55-75),
158. Tachtatzis C., Sheridan R., Michie C. *et al.* (2015) Image-based monitoring for early detection of fouling in crystallisation processes. *Chemical Engineering Science,* **133**, 82-90
159. Myerson A. (2002) *Handbook of Industrial Crystallization,* Elsevier Science
160. Braatz R.D. (2002) Advanced control of crystallization processes. *Annual Reviews in Control,* **26 I**, 87-99
161. Fujiwara M., Nagy Z.K., Chew J.W., Braatz R.D. (2005) First-principles and direct design approaches for the control of pharmaceutical crystallization. *Journal of Process Control,* **15**(5), 493-504
162. Nagy Z.K. (2009) Model based robust control approach for batch crystallization product design. *Computers and Chemical Engineering,* **33**(10), 1685-91
163. Jones A.G., Mullin J.W. (1974) Programmed cooling crystallization of potassium sulphate solutions. *Chemical Engineering Science,* **29**(1), 105-18
164. Mullin J.W., Nývlt J. (1971) Programmed cooling of batch crystallizers. *Chemical Engineering Science,* **26**(3), 369-77
165. Nagy Z.K., Braatz R.D. (2012) Advances and new directions in crystallization control. *Annual Review of Chemical and Biomolecular Engineering,* **3**, 55-75
166. Corriou J.P., Rohani S. (2008) A new look at optimal control of a batch crystallizer. *AIChE Journal,* **54**(12), 3188-206
167. Sarkar D., Rohani S., Jutan A. (2006) Multi-objective optimization of seeded batch crystallization processes. *Chemical Engineering Science,* **61**(16), 5282-95
168. Worlitschek J., Mazzotti M. (2004) Model-based optimization of particle size distribution in batch-cooling crystallization of paracetamol. *Crystal Growth and Design,* **4**(5), 891-903
169. Woo X.Y., Tan R.B.H., Chow P.S., Braatz R.D. (2006) Simulation of mixing effects in antisolvent crystallization using a coupled CFD-PDF-PBE approach. *Crystal Growth and Design,* **6**(6), 1291-303
170. Mesbah A., Huesman A.E.M., Kramer H.J.M., Van Den Hof P.M.J. (2011) A comparison of nonlinear observers for output feedback model-based control of seeded batch crystallization processes. *Journal of Process Control,* **21**(4), 652-66
171. Nagy Z.K., Chew J.W., Fujiwara M., Braatz R.D. (2008) Comparative performance of concentration and temperature controlled batch crystallizations. *Journal of Process Control,* **18**(3–4), 399-407

172. Saleemi A.N., Rielly C.D., Nagy Z.K. (2012) Comparative Investigation of Supersaturation and Automated Direct Nucleation Control of Crystal Size Distributions using ATR-UV/vis Spectroscopy and FBRM. *Crystal Growth & Design,* **12**(4), 1792-807
173. Nagy Z.K., Fevotte G., Kramer H., Simon L.L. (2013) Recent advances in the monitoring, modelling and control of crystallization systems. *Chemical Engineering Research and Design,* **91**(10), 1903-22
174. Nagy Z.K., Aamir E. (2012) Systematic design of supersaturation controlled crystallization processes for shaping the crystal size distribution using an analytical estimator. *Chemical Engineering Science,* **84**, 656-70
175. Cao Y., Kariwala V., Nagy Z.K. *Parameter Estimation for Crystallization Processes using Taylor Method.* Proceedings of the Advanced Control of Chemical Processes, 2012,
176. Nagy Z.K. (2009) Model based robust control approach for batch crystallization product design. *Computers & Chemical Engineering,* **33**(10), 1685-91
177. Threlfall T.L. (1995) Analysis of Organic Polymorphs - A Review. *Analyst,* **120**(10), 2435-60
178. Yu L., Reutzel S.M., Stephenson G.A. (1998) Physical characterization of polymorphic drugs: an integrated characterization strategy. *Pharmaceutical Science & Technology Today,* **1**(3), 118-27
179. Page T., Dubina H., Fillipi G. *et al.* (2015) Equipment and Analytical Companies Meeting Continuous Challenges May 20-21, 2014 Continuous Manufacturing Symposium. *Journal of Pharmaceutical Sciences,* **104**(3), 821-31